NBSIR 81-1652

A MEASUREMENT METHOD FOR DETERMINING THE OPTICAL AND ELECTRO-OPTICAL PROPERTIES OF A THIN FILM

Donald R. Larson

National Bureau of Standards
U.S. Department of Commerce
Boulder, Colorado 80303

December 1981

NBSIR 81-1652

A MEASUREMENT METHOD FOR DETERMINING THE OPTICAL AND ELECTRO-OPTICAL PROPERTIES OF A THIN FILM

Donald R. Larson

Electromagnetic Technology Division
National Engineering Laboratory
National Bureau of Standards
U.S. Department of Commerce
Boulder, Colorado 80303

December 1981

U.S. DEPARTMENT OF COMMERCE, Malcolm Baldrige, Secretary

NATIONAL BUREAU OF STANDARDS, Ernest Ambler, Director

CONTENTS

A Measurement Method for Determining the Optical and Electro-Optical Properties of a Thin Film

Donald R. Larson
National Bureau of Standards*
Boulder, Colorado 80303

A method of determining the complex refractive index of a thin film on a nonabsorbing substrate is developed. The optical transmittance spectrum of the structure is measured and the index is determined by matching this spectrum numerically. An iterative procedure for finding the magnitude of an induced change in refractive index is also presented. In nonabsorbing spectral regions, the index and film thickness are determined directly.

The optical transmittance of sapphire and thin films of gold and epitaxial silicon, both on sapphire, is examined. The refractive index of epitaxial silicon on sapphire, SOS, is determined and compares favorably with the results of other investigators.

The measurement method is applied to a thin film of hydrogenated amorphous silicon, a-Si:H, deposited by a capacitively coupled rf glow discharge. The index is tabulated for various wavelengths and a field induced change in index comparable to GaAs is measured.

Key Words: Electro-optic modulation; hydrogenated amorphous silicon; optical transmittance; refractive index; scattering matrix; thin film; transmittance extrema.

1. Introduction

This work shows the development of a method for determining the complex refractive index, the thickness and the change in the index with an applied voltage of a thin layer on a transparent substrate. A check of the applicability of the published refractive index values for sapphire and gold is made. The method is applied to epitaxial silicon, and the results are compared with published results of other investigators. The method is then applied to hydrogenated amorphous silicon, a-Si:H, and the index results are

*Electromagnetic Technology Division, National Engineering Laboratory.

compared with the results of another recent investigation of the same type of material. A field induced change in the index is measured and compared with other materials. A reflectance analysis is ignored due to associated experimental difficulties.

2. A Mathematical Model for the Optical Transmittance of a Planar Multilayered Structure

This section is devoted to developing a mathematical model of the optical transmittance of a multilayered thin film structure. Two mathematical approaches to the modeling are examined: the reflection coefficient and total field impedance formulation as done by Johnk [1], and the scattering matrix formulation as done by Azzam and Bashara [2]. The experimental applications to be discussed in section 3 will dictate the assumptions which can be made to simplify the model.

2.1 Wave Equation Development

The well known Maxwell equations are

$$\nabla \cdot \varepsilon \hat{\vec{E}} = \rho_v, \tag{2.1a}$$

$$\nabla \cdot \hat{\vec{B}} = 0, \tag{2.2a}$$

$$\nabla \times \hat{\vec{E}} = - \partial \hat{\vec{B}} / \partial t, \tag{2.3a}$$

and

$$\nabla \times \hat{\vec{B}}/\mu = \hat{\vec{J}} + \partial(\varepsilon \hat{\vec{E}})/\partial t. \tag{2.4a}$$

Assuming a charge-free, isotropic region with linear material parameters of ε (permittivity), μ (permeability) and σ (conductivity), Maxwell's equations may be written as:

$$\nabla \cdot \hat{\vec{E}} = 0, \tag{2.1b}$$

$$\nabla \cdot \hat{\vec{H}} = 0, \tag{2.2b}$$

$$\nabla \times \hat{\vec{E}} = - \mu \, \partial \hat{\vec{H}} / \partial t, \tag{2.3b}$$

and

$$\nabla \times \hat{\vec{H}} = \sigma \hat{\vec{E}} + \varepsilon \, \partial \hat{\vec{E}}/\partial t. \tag{2.4b}$$

Assuming further that $\hat{\vec{E}}$ and $\hat{\vec{B}}$ are in sinusoidal steady state or are complex time harmonic fields with angular frequency ω, Maxwell's equations may be rewritten as follows:

$$\nabla \cdot \vec{E} = 0, \tag{2.1c}$$

$$\nabla \cdot \vec{H} = 0, \tag{2.2c}$$

$$\nabla \times \vec{E} = -j\omega\mu\vec{H}, \tag{2.3c}$$

and

$$\nabla \times \vec{H} = j\omega(\varepsilon - j \frac{\sigma}{\omega}) \vec{E}. \tag{2.4c}$$

To obtain the wave equation, the curl of both sides of eq (2.3c) is taken.

$$\nabla \times (\nabla \times \vec{E}) = \nabla \times (-j\omega\mu\vec{H}) \tag{2.5}$$

Since the permeability μ is assumed isotropic, it is a constant with respect to the curl operation and may be moved outside along with -j and ω, resulting in eq (2.6).

$$\nabla \times (\nabla \times \vec{E}) = - j\omega\mu \, \vec{\nabla} \times \vec{H} \tag{2.6}$$

Curl of $\vec{H}$ is also related to $\vec{E}$ via eq (2.4c). Substituting the right side of eq (2.4c) into the right side of eq (2.6) yields:

$$\nabla \times (\nabla \times \vec{E}) = -j\omega\mu \, [j\omega(\varepsilon - j\frac{\sigma}{\omega})] \, \vec{E}. \tag{2.7}$$

The left side of eq (2.7) may be rewritten using a vector identity for the curl operation and the right side may be simplified algebraically. This gives

$$\nabla(\nabla \cdot \vec{E}) - \nabla^2\vec{E} = \mu\omega^2(\varepsilon - j\frac{\sigma}{\omega})\ \vec{E}. \tag{2.8}$$

Equation (2.1c) shows that the divergence of E is zero, therefore eq (2.8) becomes, after some simple alegbraic manipulation, the wave equation.

$$\nabla^2\vec{E} + \mu\omega^2(\varepsilon - j\frac{\sigma}{\omega})\ \vec{E} = 0 \tag{2.9}$$

To put eq (2.9) in a standard wave equation form, let

$$\gamma = j\omega[\mu(\varepsilon - j\frac{\sigma}{\omega})]^{1/2}, \tag{2.10}$$

and then eq (2.9) becomes

$$\nabla^2\vec{E} - \gamma^2\vec{E} = 0\ . \tag{2.11}$$

In a rectangular coordinate system, $\vec{E}$ can be represented by component unit vectors.

$$\vec{E} = \vec{a}_x E_x + \vec{a}_y E_y + \vec{a}_z E_z \tag{2.12}$$

If it is assumed that $\vec{E}$ is a uniform plane wave propagating in the z direction, (normal incidence) then $\vec{E}$ doesn't change with a change in x or y position.

$$\frac{\partial\vec{E}}{\partial x} = \frac{\partial\vec{E}}{\partial y} = 0 \tag{2.13}$$

If it is further assumed that only $E_x(z)$ exists, eq (2.11) becomes

$$\frac{d^2}{dz^2} E_x(z) - \gamma^2 E_x(z) = 0\ . \tag{2.14}$$

The solution to this second order, ordinary differential equation is well known and is given by

$$E_x(z) = E_m^{+} e^{-\gamma z} + E_m^{-} e^{\gamma z}\ . \tag{2.15}$$

It can be shown that $E_m^+ e^{-\gamma z}$ is a positive z traveling wave and thus the E_m^+ notation. Similarly, $E_m^- e^{\gamma z}$ represents a negative z traveling wave. For H_y, from eq (2.3c) and the previous assumptions

$$\frac{-\partial E_x(z)}{\partial z} = j\omega\mu H_y(z) \ . \tag{2.16}$$

In view of eq (2.15), eq (2.16) may be written as

$$H_y(z) = \frac{\gamma E_m^+ e^{-\gamma z}}{j\omega\mu} - \frac{\gamma E_m^- e^{\gamma z}}{j\omega\mu} \ . \tag{2.17}$$

The application of the above results to the total field impedance formulation and the scattering matrix formulation will now be considered.

2.2 Total Field Impedance and Reflection Coefficient Formulation

Equation (2.15) may be written as

$$E_x(z) = E_m^+ e^{-\gamma z} [1 + \Gamma(z)], \tag{2.18a}$$

where

$$\Gamma(z) = \frac{E_m^-}{E_m^+} e^{2\gamma z} \ . \tag{2.18b}$$

Since this is the ratio of the negative-going and positive-going waves, $\Gamma(z)$ is termed the reflection coefficient. Let

$$\eta = j\omega\mu/\gamma \ . \tag{2.19}$$

Now eq (2.17) may be rewritten as

$$H_y(z) = \frac{E_m^+}{\eta} e^{-\gamma z} [1 - \Gamma(z)] \ . \tag{2.20}$$

"A total-field impedance Z(z) is defined at any z location by the ratio of the total electric field to the total magnetic field" [3]. That is

$$Z_{(z)} = \frac{E_x(z)}{H_y(z)} = \eta \frac{1+\Gamma(z)}{1-\Gamma(z)} \tag{2.21}$$

Several relations will now be determined which will facilitate the calculation of the total EM-field at any location as it travels through a planar multi-layered structure. The translation of the reflection coefficient will be considered first. The reflection coefficient at a location z is denoted by $\Gamma(z)$. If another z location, z', in the same material is considered, $\Gamma(z')$ is given by

$$\Gamma(z') = E_m^- \, e^{2\gamma z'} / E_m^+, \tag{2.22}$$

and in terms of $\Gamma(z)$

$$\Gamma(z') = \Gamma(z) \, e^{2\gamma(z'-z)} \, . \tag{2.23}$$

Solving for $\Gamma(z)$ in eq (2.21) yields another useful relation.

$$\Gamma(z) = \frac{Z(z) - \eta}{Z(z) + \eta} \tag{2.24}$$

To translate across an interface, examination of the total field impedance is made. If O_1 and O_2 are two points on each side of an interface, since the tangential E and H field components are continuous across the interface or boundary, then

$$\frac{E_x(O_1)}{H_y(O_1)} = Z(O_1) = Z(O_2) = \frac{E_x(O_2)}{H_y(O_2)}. \tag{2.25}$$

Equations (2.25) and (2.24) give a means of determining the reflection coefficient on each side of a boundary.

The above formulation is now applied to a specific structure. The formulation will be used to describe the transmittance of a thin layer of a-Si:H on a sapphire (Al_2O_3) substrate (see fig. 2-1). It will be assumed that the

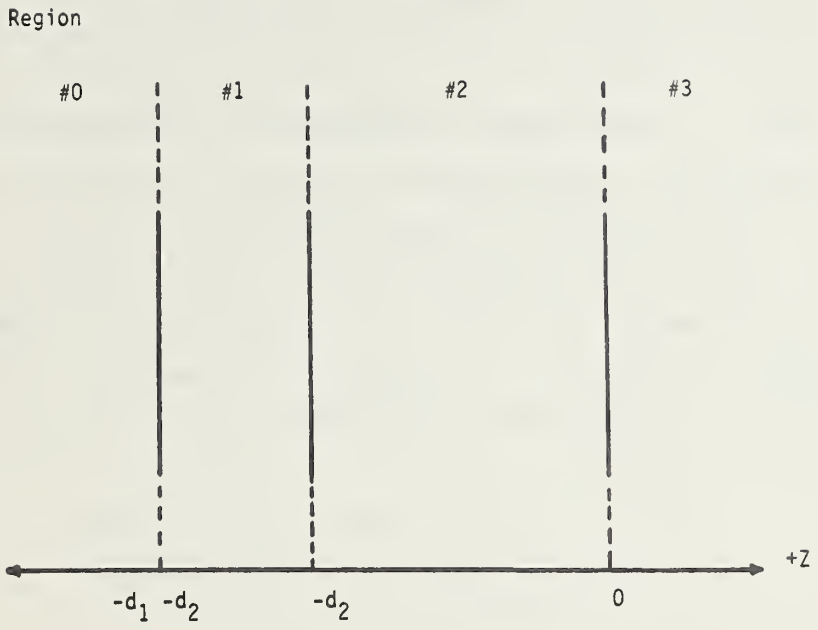

Figure 2-1. Structure for which the transmittance model is developed.

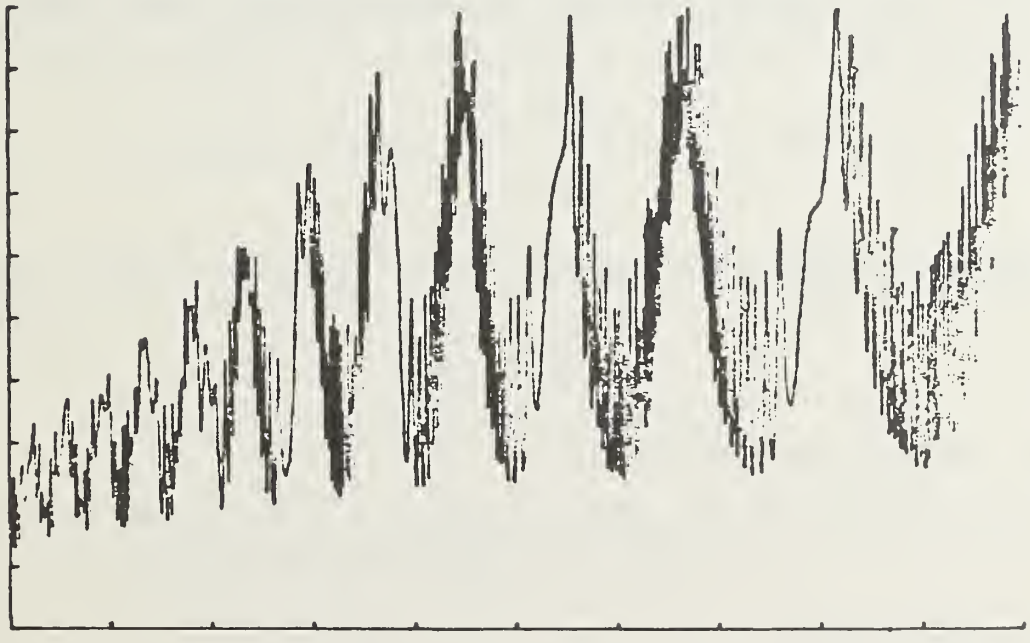

Figure 2-2. Transmittance spectrum from 0.6 to 1.2 μm. Full scale is 100 percent. Interference effects of substrate unresolvable and cause "aliasing".

interference effects in the substrate will be undetectable experimentally. The substrate's large optical thickness creates interference extrema which are less than an angstrom apart in wavelength and are thus unresolvable by the monochrometer used in this work. Also, substrate nonuniformities may "wash-out" these extrema. When a computer-generated display of the thin film extrema is plotted over several thousand angstroms, the fine structure of the substrate may cause aliasing, i.e., noisy results (see fig. 2-2) and must be removed. This removal will be accomplished by integrating the predicted transmittance over one period of the interference effects. Another method will be discussed in section 2.3. The material parameters, μ, ε, σ for optical frequencies. These are related to the complex refractive index

$$\eta = \left[\mu/\left(\varepsilon - j\frac{\sigma}{\omega}\right)\right]^{1/2} = 120\pi/(n-jk) = 120\pi/N$$

and

$$\gamma = j\ 2\pi(n-jk)/\lambda = j\ 2\pi N/\lambda\ . \tag{2.27}$$

At optical frequencies a material is usually described by n and k.

Since no material other than air is assumed present to the right of the structure depicted in figure 2-1, there will be no reflected wave and from eq (2.18b)

$$\Gamma_3(0^+) = 0\ . \tag{2.28}$$

This implies, using eq (2.24), that

$$Z_3\ (0^+) = \eta_3\ . \tag{2.29}$$

Further, from eqs (2.29) and (2.25),

$$Z_2(0^-) = Z_3(0^+) = \eta_3 \tag{2.30}$$

and this implies that

$$\Gamma_2(0^-) = \frac{\eta_3-\eta_2}{\eta_3+\eta_2}\ . \tag{2.31}$$

Then, using eq (2.23) to translate to $z = -d_2$,

$$\Gamma_2(-d_2) = \Gamma_2(0^-)\, e^{2\gamma_2(-d_2-0)} = \Gamma_2(0^-)\, e^{-2\gamma_2 d_2} \tag{2.32}$$

and hence the impedance at this location is given by

$$Z_2(-d_2) = n_2 \frac{1+\Gamma_2(-d_2)}{1-\Gamma_2(-d_2)} . \tag{2.33}$$

As noted before, at an interface

$$Z_2(-d_2^+) = Z_1(-d_2^-) \tag{2.34}$$

and so

$$\Gamma_1(-d_2^-) = \frac{Z_2(-d_2^+)-n_1}{Z_2(-d_2^+)+n_1} . \tag{2.35}$$

The above procedure is continued until $\Gamma_0(-d_1-d_2)$ is found.

If the incident EM-field is given by $Em^+{}_0$, the total field expression at the incident point is found using eqs (2.18a) and (2.18b).

$$E_{x_0}(-d_1-d_2) = E_m{}^+{}_0\, e^{\gamma_0(d_1+d_2)} [1 + \Gamma_0(-d_1-d_2)] \tag{2.36}$$

Now, since the tangential field components are continuous across an interface,

$$E_{x_0}(-d_1-d_2) = E_{x_1}(-d_1-d_2). \tag{2.37}$$

$E_m{}^+{}_1$ is then found in terms of $E_m{}^+{}_0$ from eqs (2.18) and similarly $E_m{}^+{}_2$ and $E_m{}^+{}_3$. The intermediate result is then

$$T(\lambda) = \frac{I_T}{I_0} = \left| \frac{E_{m_3}^{+}}{E_{m_0}^{+}} \right|^2 . \tag{2.38}$$

The above expression contains the description of the interference effects of the substrate. These effects are removed from the model by finding an average $T(\lambda)$ for one period of these substrate effects. This may be accomplished by using Gaussian quadrature or another numerical integrating technique. Gaussian quadrature is used in this analysis and will now be outlined. The averaged transmittance is denoted by $T_{ave}(\lambda)$ and is given by

$$T_{ave}(\lambda) = \frac{1}{\lambda_2 - \lambda_1} \int_{\lambda_1}^{\lambda_2} T(\lambda) d\lambda, \tag{2.39}$$

$$\lambda' = \frac{\lambda_1 + \lambda_2}{2}, \tag{2.29b}$$

where λ_2 and λ_1 are the wavelength locations of adjacent substrate interference maxima. Using the following change of variable,

$$\lambda = \frac{(\lambda_2 - \lambda_1)x + (\lambda_2 + \lambda_1)}{2} . \tag{2.40}$$

Equation (2.39) is changed to a standard form for Gaussian quadrature.

$$T_{ave}(\lambda) = 1/2 \int_{-1}^{1} T(x) dx \tag{2.41}$$

The integral is now approximated by a summation.

$$T_{ave}(\lambda) = 1/2 \sum_{i=0}^{n} A_i \, T(x_i) \tag{2.42}$$

"n" is specified and the A_i and x_i are given for several "n"s in table 2.1. Figure 2-3 is the resulting $T_{ave}(\lambda)$ after applying the above averaging technique to figure 2-2. The above analysis was programmed using BASIC on a mini computer and generated figures 2-2 and 2-3. The preceding analysis is more easily done in the FORTRAN computer language due to that language's complex arithmetic capabilities. A transmittance spectrum for a wavelength interval can be generated for any planar structure by the easy extension of the above analysis and using a computer to evaluate the equations.

Table 2.1

Table of Legendre Polynomials

n = 1	
$x_1 = 0$	$A_1 = 2$
n = 2	
$x_1 = -x_2 = 0.5773502692$	$A_1 = A_2 = 1$
n = 3	
$x_1 = -x = 0.7745966692$	$A_1 = A_3 = 0.55555\ldots$
$x_2 = 0$	$A_2 = 0.8888\ldots$
n = 4	
$x_1 = -x_4 = 0.8611363116$	$A_1 = A_4 = 0.3478548451$
$x_2 = -x_3 = 0.3399810436$	$A_2 = A_3 = 0.6521451549$
n = 5	
$x_1 = -x_5 = 0.9061798459$	$A_1 = A_5 = 0.2369268851$
$x_2 = -x_4 = 0.5384693101$	$A_2 = A_4 = 0.4786286705$
$x_3 = 0$	$A_3 = 0.5688888\ldots$
n = 6	
$x_1 = -x_6 = 0.9324695142$	$A_1 = A_6 = 0.1713244924$
$x_2 = -x_5 = 0.6612093865$	$A_2 = A_5 = 0.3607615730$
$x_3 = -x_4 = 0.2386191861$	$A_3 = A_4 = 0.4679139346$

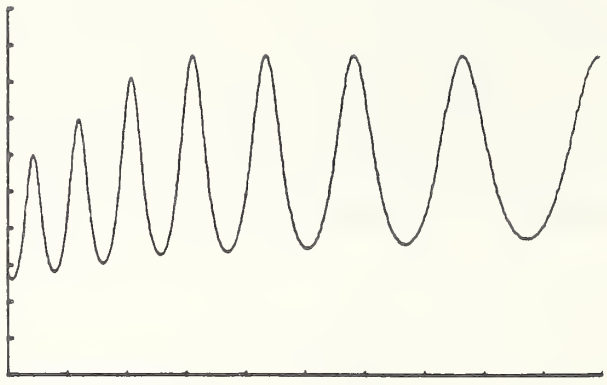

Figure 2-3. Result when the transmittance spectrum of figure 2-2 is averaged over the substrate interference period, using six point Gaussian quadrature. Full scale is 100 percent.

2.3 Scattering Matrix Formulation

The transmittance model will now be developed using the scattering matrix formulation.

Starting with eq (2.15),

$$E_x = E_m^+ e^{-\gamma z} + E_m^- e^{\gamma z} , \tag{2.15}$$

this wave equation may be rewritten as a 2x1 column matrix.

$$E_x(z) = \begin{bmatrix} E^+(z) \\ E^-(z) \end{bmatrix} \tag{2.43}$$

$E^+(z)$ is defined by

$$E^+(z) = E_m^+ e^{-\gamma z} \tag{2.44}$$

and $E^-(z)$ is defined by

$$E^-(z) = E_m^- e^{\gamma z}. \tag{2.45}$$

Since the equations used have been linear, the E field at some location z_1 can be related to the E field at another location z_2 via a 2x2 matrix transformation. Following the notation used by Azzam and Bashara [2],

$$\begin{bmatrix} E^+(z_1) \\ \\ E^-(z_1) \end{bmatrix} = \begin{bmatrix} S_{11} & S_{12} \\ \\ S_{21} & S_{22} \end{bmatrix} \begin{bmatrix} E^+(z_2) \\ \\ E^-(z_2) \end{bmatrix} \tag{2.46}$$

with matrix S called the scattering matrix.

To specialize the S matrix to an interfacial region, let z_1 and z_2 be on either side of an interface. For this special case, S will be renamed I. The elements of matrix I may be found by considering the system depicted in figure 2-4. The matrix representation of this system is as follows, dropping the z variable notation in favor of subscripts

$$\begin{bmatrix} E_1^+ \\ \\ E_1^- \end{bmatrix} = \begin{bmatrix} I_{11} & I_{12} \\ \\ I_{21} & I_{22} \end{bmatrix} \begin{bmatrix} E_2^+ \\ \\ 0 \end{bmatrix}. \tag{2.47}$$

When eq (2.47) is expanded, it is seen that

$$E_1^+ = I_{11}\, E_2^+ \tag{2.48a}$$

$$E_1^- = I_{21}\, E_2^+ \ , \tag{2.48b}$$

but using the Fresnel reflection and transmission coefficients defined by

$$E_1^+ = 1/r_{12}\, E_1^- \tag{2.49}$$

$$E_1^+ = 1/t_{12}\, E_2^+ \tag{2.50}$$

yields the following results.

$$I_{11} = 1/t_{12} \tag{2.51}$$

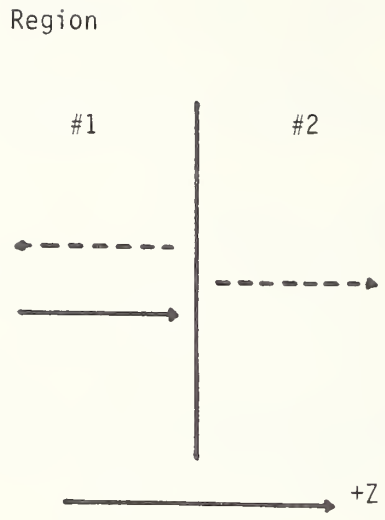

Figure 2-4. System used in the determination of the interface matrix elements I_{11} and I_{21}.

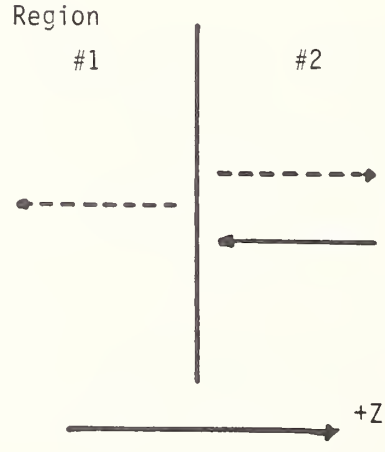

Figure 2-5. System used in the determination of the interface matrix elements I_{12} and I_{22}.

$$I_{21} = \frac{r_{12}}{t_{12}} \tag{2.52}$$

To find I_{22} and I_{12}, the direction of propagation assumed in figure 2-4 is simply reversed (see fig. 2-5). The matrix representation of this new system is

$$\begin{matrix} 0 \\ \\ E_1^- \end{matrix} = \begin{matrix} I_{11} & I_{12} \\ \\ I_{21} & I_{22} \end{matrix} \begin{matrix} E_2^+ \\ \\ E_2^- \end{matrix} \tag{2.53}$$

The applicable Fresnel coefficients are now given by eqs (2.54) and (2.55).

$$E_2^+ = r_{21}\, E_2^- \tag{2.54}$$

$$E_1^- = t_{21}\, E_2^- \tag{2.55}$$

When the matrix product in eq (2.53) is performed, relations (2.56) and (2.57) result.

$$I_{11}E_2^+ + I_{12}E_2^- = 0 \tag{2.56}$$

$$I_{21}E_2^+ + I_{22}E_2^- = E_1^- \tag{2.57}$$

Some algebra and the use of the Fresnel coefficient identities found in [4],

$$t_{21} = \frac{1-r_{12}^2}{t_{12}} \tag{2.58}$$

and

$$r_{21} = -r_{12} \tag{2.59}$$

gives the following results

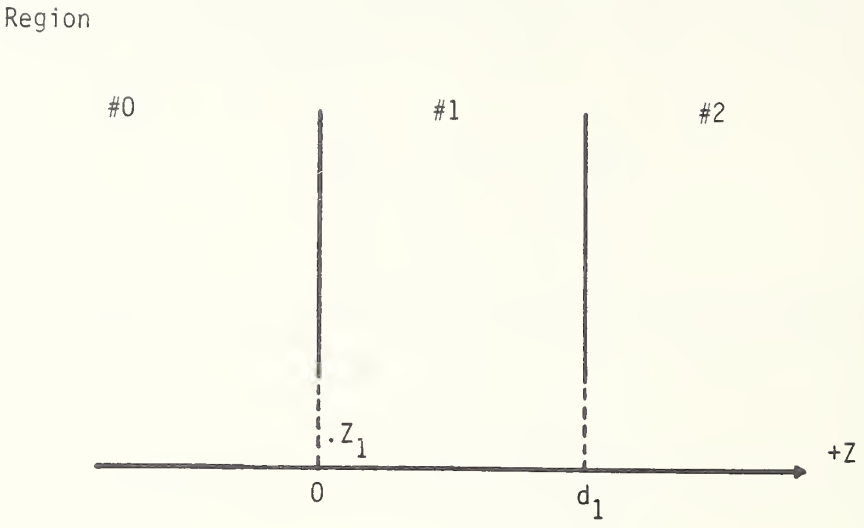

Figure 2-6. System used in the determination of the interface matrix elements.

$$I_{12} = \frac{r_{12}}{t_{12}} \tag{2.60}$$

$$I_{22} = \frac{1}{t_{12}} . \tag{2.61}$$

The interface matrix, I, is now completely determined and is given by

$$I = \frac{1}{t_{12}} \begin{bmatrix} 1 & r_{12} \\ r_{12} & 1 \end{bmatrix} . \tag{2.62}$$

Matrix S is also called the layer matrix L if the system under consideration consists of locations z_1 and z_2 that are at either end of an isotropic layer. Figure 2-6 illustrates this system and eq (2.63) describes it.

$$\begin{bmatrix} E_1^+ \\ \\ E_1^- \end{bmatrix} = \begin{bmatrix} L_{11} & L_{12} \\ \\ L_{21} & L_{22} \end{bmatrix} \begin{bmatrix} E_2^+ \\ \\ E_2^- \end{bmatrix} \tag{2.63}$$

Performing the matrix multiplication indicated on the right side of eq (2.63) give eqs (2.64) and (2.65).

$$E_1^+ = L_{11}\, E_2^+ + L_{12}\, E_2^- \tag{2.64}$$

$$E_1^- = L_{21}\, E_2^+ + L_{22}\, E_2^- \tag{2.65}$$

Equations (2.44) and (2.45) for $z = z_1$ and $z = z_2$ yield

$$E_m^+ e^{-\gamma z_1} = L_{11} E_m^+ e^{-\gamma z_2} + L_{12}\, E_m^- e^{\gamma z_2} \tag{2.66}$$

and

$$E_m^- e^{\gamma z_1} = L_{21}\, E_m^+ e^{-\gamma z_2} + E_m^- e^{\gamma z_2} \quad . \tag{2.67}$$

The layer matrix under consideration must be valid for any isotropic layer. L_{11} and L_{21} may be found if the assumption is made that the layer is infinite and only a forward traveling (positive z traveling) wave is present. That is,

$$E_1^- = E_2^- = 0 \quad . \tag{2.68}$$

Using these two conditions with eqs (2.66) and (2.67) yields

$$E_m^+ e^{-\gamma z_1} = L_{11}\, E_m^+ d^{-\gamma z_2} \tag{2.69}$$

and

$$0 = L_{21}\, E_m^+ e^{-\gamma z_2} \quad . \tag{2.70}$$

These two equations reduce to

$$L_{11} = e^{-\gamma(z_1-z_2)} = e^{\gamma d} \tag{2.71}$$

and

$$L_{21} = 0 \ . \tag{2.72}$$

Similarly, L_{12} and L_{22} may be found if the assumption is made that the layer is again infinite but only a negative z traveling wave exists. The results are

$$L_{12} = 0 \tag{2.73}$$

$$L_{22} = e^{\gamma(z_1-z_2)} = e^{-\gamma d} \ . \tag{2.74}$$

All elements of the layer matrix have been determined and L is given by

$$L = \begin{bmatrix} e^{\gamma d} & 0 \\ 0 & e^{-\gamma d} \end{bmatrix} \ , \tag{2.75}$$

and γ can again be defined as

$$\gamma = j\ 2\pi\ N/\lambda \ . \tag{2.27}$$

Any multilayered structure can now be described by using the product of the interface and layer matrices to give the scattering matrix. This formulation is now applied to thin layer of a-Si:H on a lossless sapphire substrate. Originally, the substrate will be considered semi-infinite and later the effect of the substrate-air interface will be included.

This will be done in such a manner as to neglect the substrate interference effects. This structure (see fig. 2-7) may be described by eq (2.46) with matrix S given by

$$S = I_{12}\ L_2\ I_{23}, \tag{2.76}$$

with

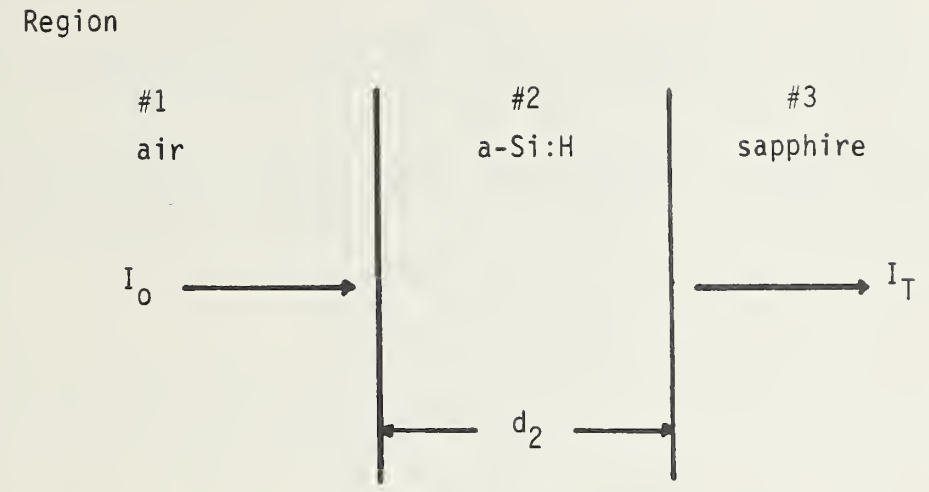

Figure 2-7. Thin film on an infinite substrate.

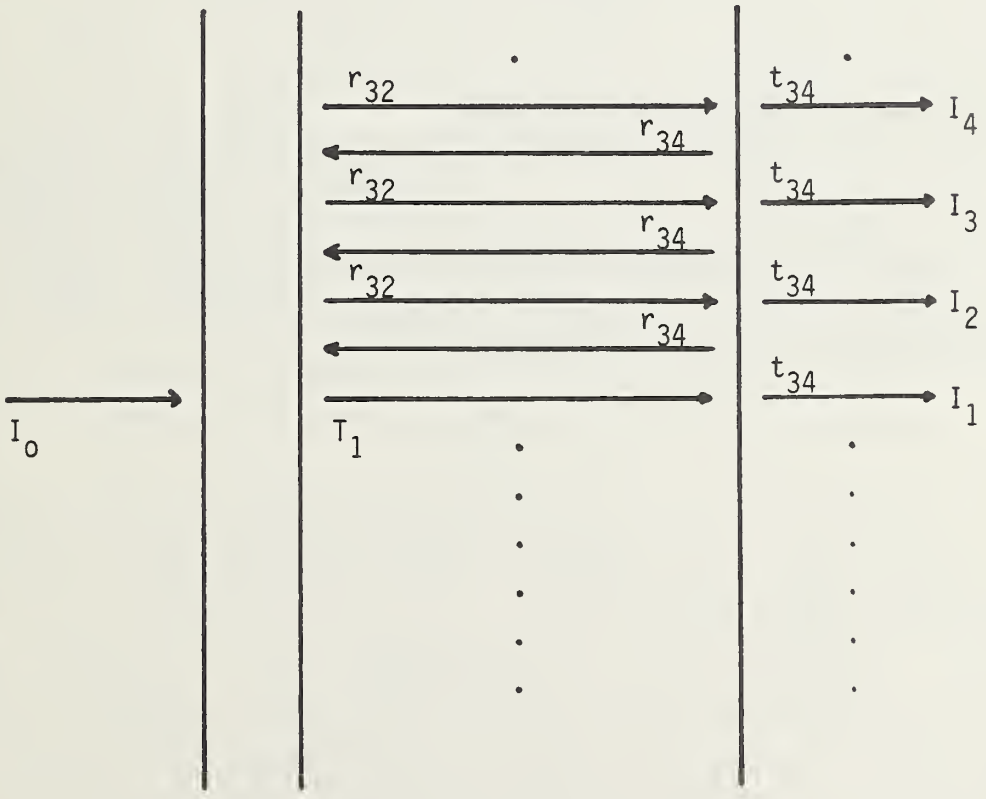

Figure 2-8. Thin film on a finite substrate. Rays used in geometrical optics analysis portrayed.

$$I_{12} = \frac{1}{t_{12}} \begin{bmatrix} 1 & r_{12} \\ r_{12} & 1 \end{bmatrix}, \tag{2.77}$$

$$L_2 = \begin{bmatrix} e^{\gamma_2 d_2} & 0 \\ 0 & e^{-\gamma_2 d_2} \end{bmatrix}, \tag{2.78}$$

and

$$I_{23} = \frac{1}{t_{23}} \begin{bmatrix} 1 & r_{23} \\ r_{23} & 1 \end{bmatrix}. \tag{2.79}$$

The transmittance of this structure is given by relation (2.80).

$$T_1 = \left| \frac{E_3^+}{E_1^+} \right|^2 = \frac{1}{S_{11}\, S_{11}^*} \tag{2.80}$$

The asterisk denotes the complex conjugate.

From previous assumptions, the substrate may be analyzed using geometrical optics, therefore to "fold-in" the effects of the substrate-air interface, ray tracing and the Fresnel coefficients are used for the EM radiation in the substrate. I denotes intensity in figure 2-8. The total transmitted intensity is the infinite sum of I_1, I_2, ...

$$I_T = \sum_{j=1}^{\infty} I_j. \tag{2.81}$$

T_1 is the transmittance for an infinite substrate and I_1, I_2, etc. can be found using the Fresnel coefficients.

$$I_1 = I_0\, T_1 \left| t_{34} \right|^2 \tag{2.82}$$

$$I_2 = I_0\, T_1 \left| r_{34}\, r_{32}\, t_{34} \right|^2 \tag{2.83}$$

It can be written as

$$I_T = I_0\, T_1 \left|t_{34}\right|^2 \left[1 + \left|r_{34}\, r_{32}\right|^2 + \left|(r_{34}\, r_{32})^2\right|^2 + \cdots\right] , \tag{2.84}$$

where the expression inside the brackets is a geometric series which may be summed to give eq (2.85) for I_T.

$$I_T = \frac{I_0 T_1 |t_{34}|^2}{1 - |r_{34} r_{32}|^2} \tag{2.85}$$

The total average transmittance is then

$$T_{ave} = \left|\frac{I_T}{I_0}\right|^2 = T_1 \frac{|t_{34}|^2}{1 - \left|r_{34}\, r_{32}\right|^2} \quad . \tag{2.86}$$

The matrix S can be extended to any arbitrary multilayered structure by annexing I and L matrices. The above analysis is readily programmed using BASIC or FORTRAN to provide a transmittance spectrum for any wavelength interval for which the material parameters, n, k and thickness, are available. Such a FORTRAN program appears in appendix A.

It should be noted that either integrating out the substrate interference effects or neglecting them via the ray tracing technique may be applied to either formulation and are mathematically equivalent under the assumptions of this section. Either formulation may be used for determining the optical constants of a layer, which will be considered in the next section.

3. Determination of the Optical Parameters of a Thin Film Exhibiting Interference Extrema

This section outlines a method for determining the complex refractive index and thickness of a single thin film on a lossless substrate, from its transmittance spectrum. The method is based on the transmittance model developed in section 2 and requires that the material thickness be large enough so that transmittance extrema are present in the spectral region of interest. If the material under examination has zero or immeasurably low absorption in a particular wavelength region, several major simplifications may be made in the model.

3.1 Determining Index of Refraction and Thickness in a Spectral Region of Zero Absorption

The structure under consideration appears in figure 3-1. It is assumed that the layer and its substrate are lossless and that the layer is sufficiently thick to exhibit interference caused transmittance extrema. Using the scattering matrix formulation, the averaged transmittance, T_{ave}, is given by eq (3.1a), where S is given by eq (3.1b) (also refer to section 3.2).

$$T_{ave} = \frac{T_1 T_2}{1-R_2 R_3}, \tag{3.1a}$$

where

$$S = I_{01}\, L_1\, I_{12}, \tag{3.1b}$$

$$T_1 = \frac{1}{S_{11} S_{11}^*}, \tag{3.2a}$$

$$T_2 = t_{23}\, t_{23}^*, \tag{3.3a}$$

$$R_2 = r_{23}\, r_{23}^*, \tag{3.4a}$$

and

$$R_3 = \frac{S_{12} S_{12}^*}{S_{11} S_{11}^*} \quad . \tag{3.5a}$$

For the optical system depicted in figure 3-1, eqs (3.2a) through (3.5a) become

$$T_1 = \frac{16 n_0^2 n_1^2}{(n_0+n_1)^2(n_1+n_2)^2 + (n_0-n_1)^2(n_1-n_2)^2 + 2(n_0^2-n_1^2)(n_1^2-n_2^2)\cos\left(\frac{4\pi n_1 d_1}{\lambda}\right)}, \tag{3.2b}$$

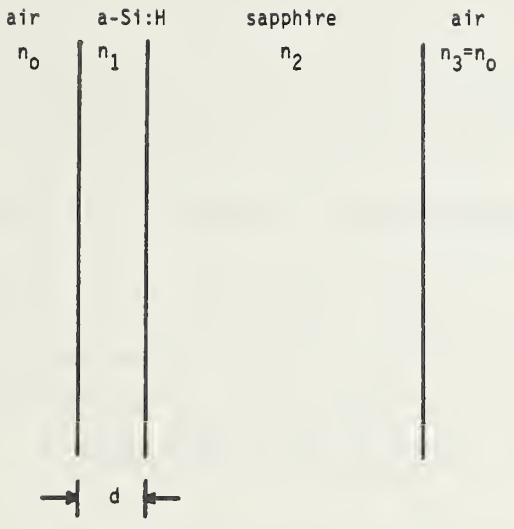

Figure 3-1. Structure depicting a thin film on a thick but finite substrate. Note labeling of material regions.

$$T_2 = \frac{4n_2^2}{(n_2+n_0)^2}, \tag{3.3b}$$

$$R_2 = \left(\frac{n_2-n_0}{n_2+n_0}\right)^2, \tag{3.4b}$$

and

$$R_3 = \frac{(n_0+n_1)^2(n_1-n_2)^2 + (n_0-n_1)^2(n_1+n_2)^2 + 2(n_0^2-n_1^2)(n_1^2-n_2^2)\cos(\frac{4\pi n_1 d_1}{\lambda})}{(n_0+n_1)^2(n_1+n_2)^2 + (n_0-n_1)^2(n_1-n_2)^2 + 2(n_0^2-n_1^2)(n_1^2-n_2^2)\cos(\frac{4\pi n_1 d_1}{\lambda})}. \tag{3.5b}$$

Since T_{ave} is a function of wavelength, its spectral extrema may be found by differentiating eq (3.1a) with respect to wavelength and letting the result go to zero. For the case when the refractive index of the layer (n_1) is greater than that of the substrate (n_2), relations (3.6) and (3.7) result when $dn/d\lambda$ is zero.

$$\text{For a maximum } 2n_1d = m\lambda \quad m = 0, 1, 2, \cdots. \tag{3.6}$$

$$\text{For a minimum } 2n_1d = (m+1/2)\lambda \quad m = 0, 1, 2\cdots. \tag{3.7}$$

If n_1 is less than n_2, relation (3.6) applies for transmittance minima and eq (3.7) applies for transmittance maxima. For the materials examined in this work, n_1 is greater than n_2. If eq (3.7) is substituted into the cosine terms in the expressions for T_1 and R_3, it is seen that:

$$\cos \frac{4nd\pi}{\lambda} = \cos ((2m+1)\pi) = -1 \quad . \tag{3.8}$$

This allows $T_{ave}(min)$ to be reduced algebraically to

$$T_{ave}(min) = \frac{4n_0n_1{}^2n_2}{n_0{}^2n_1{}^2 + n_0{}^2n_2{}^2 + n_1{}^4 + n_1{}^2n_2{}^2} \quad . \tag{3.9}$$

The intermediate steps leading to eq (3.9) may be found in appendix B. This implies that the unknown index, n_1, may be determined directly from $T_{ave}(\lambda min)$, if the substrate refractive index is known. Solving for n_1 yields

$$n_1 = \left\{\frac{1}{2}\left[-(n_0{}^2 - 4n_0n_2/T + n_2{}^2) + [(n_0{}^2-4n_0n_2/T + n_2{}^2)^2 - 4n_0{}^2n_2{}^2\right]^{1/2}\right\}^{1/2}. \tag{3.10}$$

It should be noted that the above expression for n_1 is not dependent on m, the order of the extremum or the layer thickness. If m is known, the thickness of the layer may be found using eq (3.7) in a rearranged form and using the n_1 just determined.

$$d = \frac{(m+1/2)\lambda}{n_1} \tag{3.11}$$

Appendix C examines the error introduced in the index determination of a dispersive material when eq (3.7) is used, an often negligible error.

The analysis in section 2, coupled with the simplifying assumptions of this section, allowed an expression for n_1 to be found in terms of n_0, n_2 and T_{ave} (min). It is useful to note that no information on n_1 is found if the previous analysis is carried out using T_{ave} (max) instead of T_{ave} (min). The resulting expression is:

$$T_{ave}\ (\text{max}) = \frac{2n_0n_2}{n_0{}^2+n_2{}^2}\ . \tag{3.12}$$

Equation (3.12) is valuable in checking the experimental procedure and data. The peak experimental transmittance should agree with the value given by eq (3.12). The amount of agreement is a quality measure for the experimental data.

3.2 Determining the Optical Parameters of an Absorbing Layer

A determination of the optical constants of an absorbing layer requires the layer thickness to be known. Many optical and semiconductor materials are optically transparent in some spectral region and the procedure outlined in section 3.1 may be used to determine the layer thickness. A nonzero k causes the interference minimums to shift to shorter wavelengths and the maximums to shift to longer wavelengths. If n is approximately 3.7, a value of k greater than 0.05 causes a shift of 10 Å in extrema location, one which may be experimentally resolvable. If k is less than 0.02, the location of the extrema can still be determined by eqs (3.6) and (3.7), as the shift is less than 10 Å and may be unresolvable.

For this work, it will be assumed that the thickness d can be determined via the procedure outlined in the previous section. That is, the material under examination is not absorbing in a particular wavelength region and eqs (3.10) and (3.11) can be used. With the thickness and order determined, the

complex refractive index can be determined in the wavelength region of interest via an iterative procedure. This procedure is now outlined.

The transmittance spectrum of the structure must be observed and recorded for the particular wavelength region desired and must exhibit extrema. Equations (3.6) and (3.7) are used to find values of "n" at the extrema locations and these values may be extended to wavelengths between extrema via linear interpolation. A theoretical transmittance spectrum is then calculated. The peak amplitude of the synthesized and experimental transmittances are compared and the value of k is adjusted to increase the agreement. If the value of k is increased, the peak transmittance will decrease. "n" may also be adjusted to account for a possible shift in extrema position due the adjustment of k and to increase the agreement in extrema location. An increase in n causes the extrema to shift to longer wavelengths. A new transmittance spectrum is calculated with the revised n and k and again compared to the experimental data. The process is repeated until the theoretical and experimental agreement is within the error of the experimental data measurement.

Goodman [5] has observed that the peak-to-valley ratio of the transmittance spectrum may be used to determine n if both the layer and substrate are lossless and nondispersive. Although these two restrictions are not made here, the peak-to-valley ratio as well as the extrema position may be used as an agreement criteria for the experimental and theoretical transmittance comparison.

The above iterative procedure may be programmed or done by hand although the transmittance spectrum calculation is best done using a computer.

Determination of n and k can also be done for a layer buried in a multilayered structure via the preceding iterative method. The other layers need to be well characterized and the layer under examination must be of known thickness. The initial guess for n from eqs (3.6) and (3.7) may be further from its actual value but more iterations resolve this complication.

In concluding this section, it should be pointed out that the determination of the layer thickness is very critical. Denton, Campbell and Tomlin [6] point out that in Tomlin's method of determining n and k from reflectance and transmittance measurements, a 5 percent error in the layer thickness can make the results far from reasonable. The same thing is true for the procedure outlined in this section, particularly when applied to multilayered structures.

3.3 Determining the Magnitude of an Induced Change in the Complex Refractive Index

The model developed in section 2 may be used to calculate a theoretical transmittance spectrum of a stratified structure consisting of an arbitrary number of layers. If the complex refractive index of one of those layers is changed slightly, the transmittance spectrum will also change. This section will outline a procedure for determining this change in index from a change in the transmittance spectrum. The change in index will be assumed to have been accomplished by the application of energy to the structure.

The "modulation spectrum" will be defined as follows,

$$M = \frac{T-T_W}{T} . \tag{3.13}$$

T is the transmittance without applied energy and T_W is the transmittance when energy is being applied to the structure.

Finding the change in n and k is done via an iterative process. The iterative process involves generating a modulation spectrum from an initial guess of the change in index and comparing the resulting theoretical modulation spectrum with the experimental modulation spectrum. The changes in n and k are then adjusted to increase the agreement between experiment and theory and a new modulational spectrum is calculated. This new spectrum is compared to experiment. This process is repeated until the desired agreement is achieved and the values for the change in n and k are determined.

Figure 3-2 illustrates a modulation spectrum from a layer showing interference effects (see fig. 3-3). A change in k results in amplitude modulation as the absorptance changes. This effect may be seen in figure 3-2 at the shorter wavelength end of the spectrum. A change in n causes a shift in the interference peaks and phase modulation results. This is the dominant effect seen at longer wavelengths in figure 3-2. These observations aid the programmer in using the iterative process.

4. A Comparison of Calculated and Experimental Transmittance Spectra, Values of Refractive Index, and Thickness

This section outline the procedures followed to compare experimentally determined transmittance spectra of sapphire and of gold on sapphire with the transmittance spectrum of each, calculated from the scattering matrix model

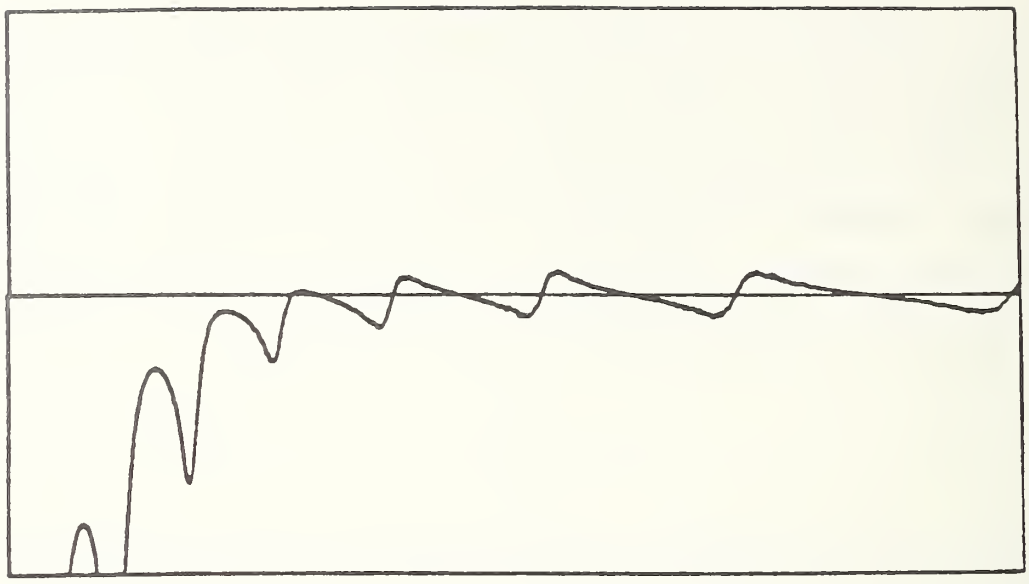

Figure 3-2. Calculated modulation spectrum from 0.6 to 1.2 μm.

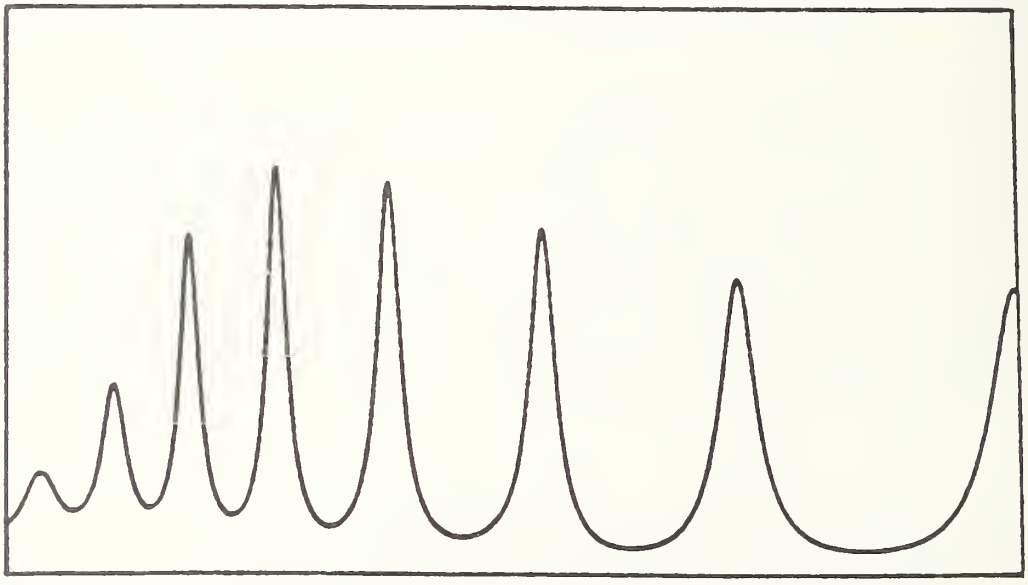

Figure 3-3. Calculated transmittance spectrum from 0.6 to 1.2 μm.

developed in section 2. These calculations are made using values of refractive index from the literature. The comparison of calculated with experimental transmittance provides a check of the applicability of the published refractive index data of these two materials with the actual refractive index of the materials used in this work.

The experimental procedure and the results obtained when the measurement method is applied to an epitaxial silicon layer is also described. The index of refraction results are compared with published values and the thickness result is compared with a measurement made with a surface profilometer. This provides a verification of the measurement method.

4.1 Comparison of an Experimentally and Theoretically Determined Transmittance Spectrum of a Sapphire Wafer

A sapphire wafer is used as the substrate of every structure considered in this work, and its measured transmittance spectrum should agree with a theoretical spectrum calculated from published index data. By comparing the measured spectra with the calculated spectra based on published data, some idea of the experimental limitations is obtained.

The physical dimensions of the substrate were 0.635 cm x 0.635 cm x 0.0254 cm and the sample was provided polished on both sides. A transmittance spectrum from 0.6 to 1.2 μm is considered here. Figure 4-1 is a schematic of the experimental setup. A minicomputer is used to control the grating monochrometer wavelength setting, take and store the data, and provide a plot and printout of the results. Reflective optics are used to focus the light from the tungsten source into and as it emerges from the monochrometer. By using reflective optics, the focal point is constant with wavelength which minimizes the effort needed to keep the light focused on the sample and the detector throughout the spectral range examined. A silicon p-n junction detector is used in conjunction with a lock-in amplifier to obtain the data. The analog signal is processed by an A-D converter and sent to the computer. Figure 4-2 is a plot of the incident spectrum (I), the transmitted spectrum (T), and the ratio of these two or the transmittance spectrum (N). The minicomputer was then programmed in BASIC to calculate a transmittance spectrum using the scattering matrix formulation of the model. The refractive index used for sapphire was obtained from the supplier and was originally determined by I. H. Malitson [7]. Figure 4-3 is a plot of the calculated

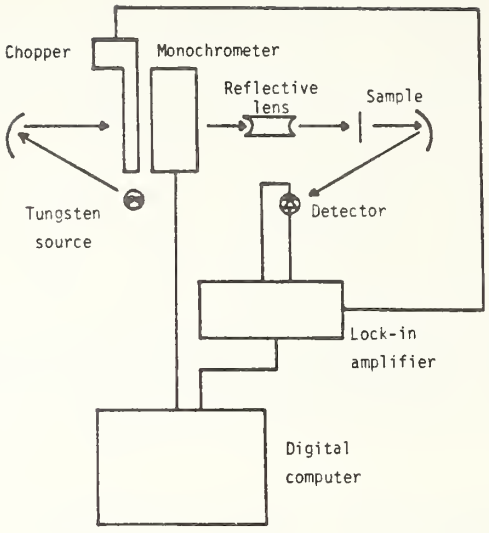

Figure 4-1. Equipment array used to obtain experimental transmittance spectra.

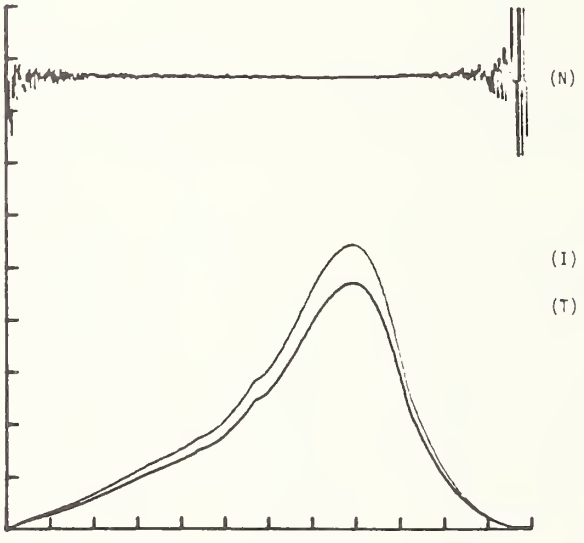

Figure 4-2. (I) incident, (T) transmitted, (N) transmittance of sapphire from 0.6 to 1.2 μm. Transmittance (N) full scale is 100 percent.

spectrum made to the same scale as the plot of the experimental transmittance spectrum, figure 4-2(N).

The experimental and theoretical spectra agree extremely well in the region where a good signal-to-noise ratio exists. The published values of index for sapphire are concluded to be in good agreement with the actual index of the sapphire wafer used.

4.2 Gold on Sapphire Transmittance Comparison

In section 5 the modulator structure will be modeled. This structure consists of an a-Si:H layer sandwiched by two gold films with a sapphire substrate. Since the gold films are thin enough to be semitransparent, 200 Å each, the refractive index is dependent on the rate of deposition [8]. To model the modulator transmittance, the transmittance of the gold layers must be known.

A 200 Å film of gold was deposited on a sapphire wafer and the transmittance of this structure was obtained following the procedure outlined in section 4.1. Figure 4-4 is a plot of the incident (I), transmitted (T), and transmittance (N) spectra from 0.6 to 1.2 μm. The transmittance was then compared to a transmittance spectrum plotted using the model and refractive index data from the literature [9]. The transmittance amplitude and structure were initially in reasonable agreement but to increase the agreement, the thickness was decreased to 185 Å and the imaginary part of refractive index was changed. Several iterations of changing the index parameter, "k", and comparing theoretical and the experimental transmittance spectra produced a theoretically generated plot which is in good agreement with experiment (see fig. 4-5). The refractive index data used to generate figure 4-5 is listed in table 4.1 (DL) along with data published by Heavens [10] and Weiss [9]. The variation in refractive index, "k", is an indication that the gold layers used in the modulator should be examined on each modulator device, the "k" appears to be very deposition process dependent. The examination of the gold film on sapphire will be understood to be part of the experimental procedure in the examination of the modulator structure in section 5.

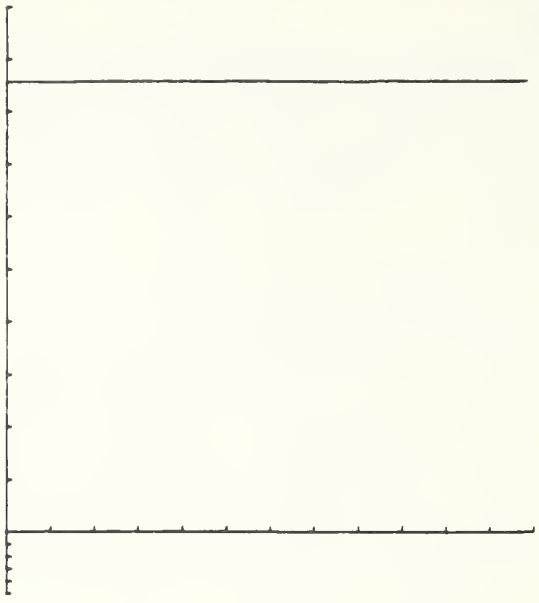

Figure 4-3. Calculated transmittance spectrum from 0.6 to 1.2 μm for sapphire. Full scale is 100 percent.

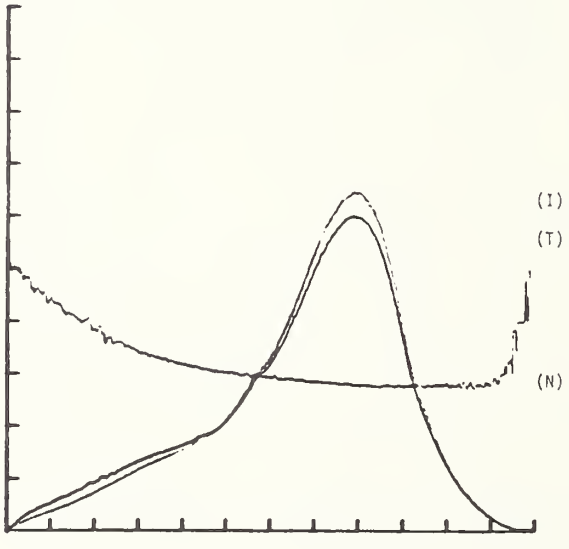

Figure 4-4. Gold on sapphire experimental spectra from 0.6 to 1.2 μm. (I) incident, (T) transmitted, (N) transmittance. Transmittance (N) full scale is 100 percent. The (T) scale is 33% of the (I) scale.

4.3 Comparison of Refractive Index Values of Epitaxial Silicon from 0.6 to 1.6 μm

A comparison of epitaxial silicon on sapphire (SOS) with hydrogenated amorphous silicon on sapphire (a-Si:H) is of general interest due to their physical similarities and applications. The rough, uncoated side of an SOS wafer was polished using a polishing wheel and a diamond slurry. Four samples, 0.635 cm square by approximately 0.0254 cm thick were thus processed. The silicon was etched from one of these samples and a transmittance spectrum was observed and compared with the calculated sapphire spectrum. Good agreement is seen when figures 4-6 and 4-2 are compared, indicating the polishing described above is sufficient. The transmittance spectrum of an SOS sample was then obtained using the same experimental procedure as outlined in section 4.1 and in figure 4-1. The results are plotted in figure 4-7 for the 0.6 to 1.2 μm range and in figure 4-8 for the 1.0 to 1.6 μm range. Both figures depict the incident (I), transmitted (T) and transmittance (N) spectra. A germanium p-n junction detector was used for both spectra and was required for the 1.0 to 1.6 micrometer range as silicon detectors cut off around 1.2 μm.

Table 4.1
Refractive Index of Gold

	Weiss		DL		Heavens	
λ μm	n	k	n	k	n	k
.603	.2	2.9	.2	2.78	.23	2.97
.65	.165	3.37	.165	3.37	.19	3.5
.7	.13	3.84	.13	3.84	.17	3.97
.75	.14	4.245	.14	4.2	.16	4.42
.8	.15	4.65	.15	4.55	.16	4.84
.85	.16	4.995	.16	4.8	.17	5.30
.9	.17	5.34	.17	5.0	.18	5.72
.95	.175	5.69	.175	5.2	.19	6.10
1.0	.18	6.04	.18	5.4	*	*
1.25	.27	7.33	.27	6.25	*	*

Table 4.2

Refractive Indices of Epitaxial Silicon

	DL		Hulthen		Kühl et al.	
λ μm	n	k	n	k	n	k
1.543	3.3900	0	*	*	3.458	*
1.405	3.3956	0	*	*	3.466	*
1.298	3.4221	.0005	*	*	3.474	*
1.2	3.4274	.0010	*	*	3.483	*
1.123	3.4542	.0014	*	*	3.495	*
1.052	3.4669	.0020	3.54	.0012	3.508	*
.992	3.4871	.0026	3.55	.0029	3.526	*
.938	3.5034	.0034	3.56	.0046	3.540	*
.893	3.5315	.0043	3.58	.0073	3.554	*
.848	3.5399	.0061	3.60	.0112	3.569	*
.813	3.5724	.0079	3.63	.0119	3.582	*
.777	3.5849	.0092	3.66	.0141	3.596	.0102
.749	3.6203	.01	3.68	.0171	3.626	.011
.722	3.6484	.0118	3.71	.0199	3.65	.0125

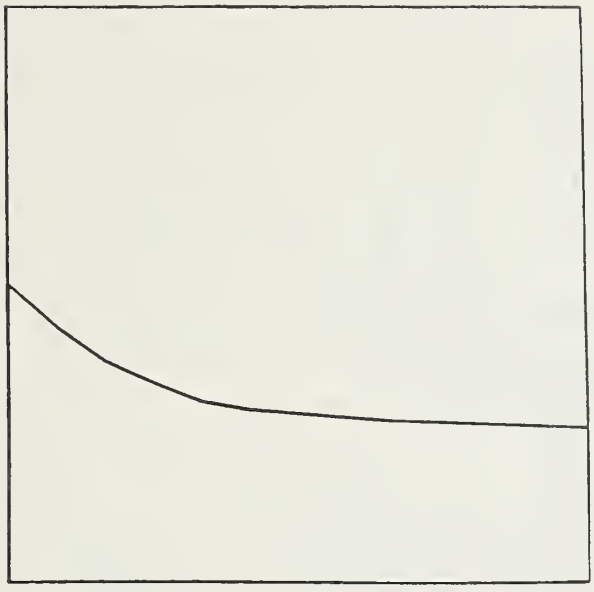

Figure 4-5. Calculated gold on sapphire transmittance spectrum from 0.6 to 1.2 μm. Full scale is 100 percent.

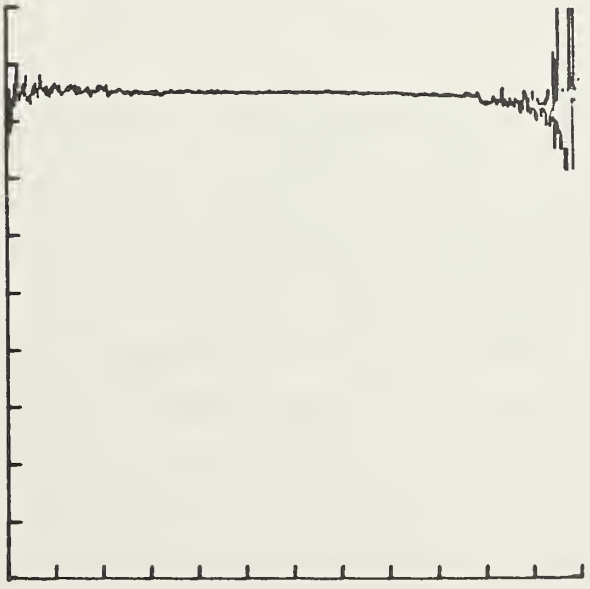

Figure 4-6. Experimental transmittance spectrum of sapphire from 0.6 to 1.2 μm. Full scale is 100 percent.

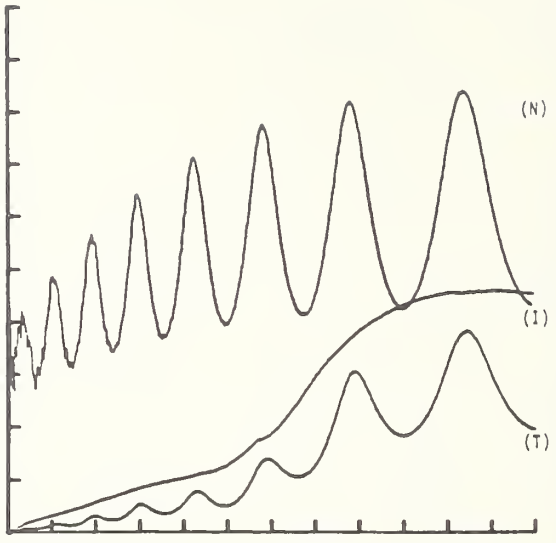

Figure 4-7. Experimental SOS spectra from 0.6 to 1.2 μm. Transmittance (N) full scale is 100 percent.

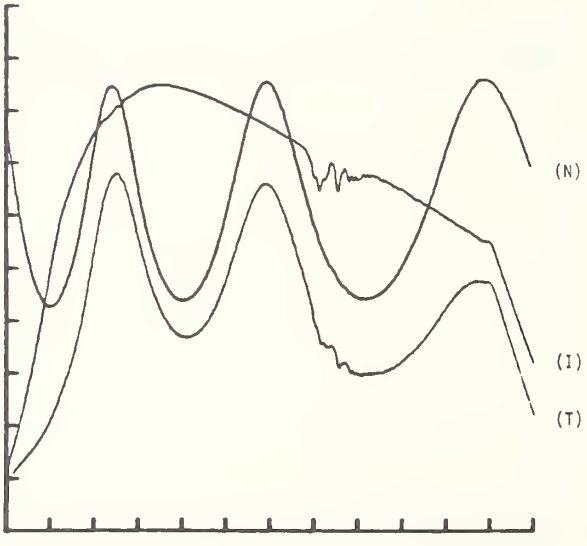

Figure 4-8. Experimental SOS spectra from 1.0 to 1.6 μm. Transmittance (N) full scale is 100 percent.

In examining these transmittance spectra, eq (3.12) is useful. In a non-absorbing region of the spectrum, eq (3.12) is applicable and may be used to indicate which spectral regions are actually absorbing and which are not. The spectral regions where eq (3.10) may be used are thus determined. Equation (3.10) is then used to calculate the refractive index of the silicon at the wavelength of a transmittance minimum. The results obtained by following the above procedure and the measurement method outlined in section 3 are listed in table 4.2 along with the published results of other investigators, [11,12]. The transmittance spectrum illustrated in figure 4-7 shows definite absorption effects in the region from 0.6 to 0.95 μm. Since the imaginary part of the refractive index, k, is nonzero, the iterative method outlined in section 3 must be employed for the 0.6 to 0.95 μm region. This was done on a computer using the FORTRAN language, a graphics terminal, hard copy unit, and PLOT-10 plotting software. The results are also listed in table 4.2, along with the results of the other investigators. For the real part of the refractive index, n, Hulthen [11] and Kühl et al. [12] agree to 1.5 percent, and both agree with the results presented here to 2 percent. For the imaginary part of the index of refraction, Hulthen and Kühl only agree to 37 percent, and they agree with the present results to 69 percent. The absorption, and thus the k, is very material dependent so the above agreement is still considered reasonable.

4.4 Comparison of Two Thickness Determinations

The documentation provided with the SOS sample states that the silicon layer is approximately 1 μm thick. The thickness of the sample examined above was calculated from the index n determined at a wavelength of 1.405 μm using eq (3.7). The order, m, was required for this calculation and was determined by assuming the index was nondispersive in the spectral region from the transmittance minimum at 1.405 μm to the transmittance maximum at 1.543 μm. Equations (3.6) and (3.7) can be combined and yield eq (4.2) for an adjacent transmittance minimum and maximum.

$$(m + 1/2)\ \lambda_v = m\ \lambda_p \tag{4.2}$$

From eq (4.2), m, an integer, is found to be 5 for the transmittance peak located at 1.543 μm. The v and p subscripts in eq (4.2) indicate the

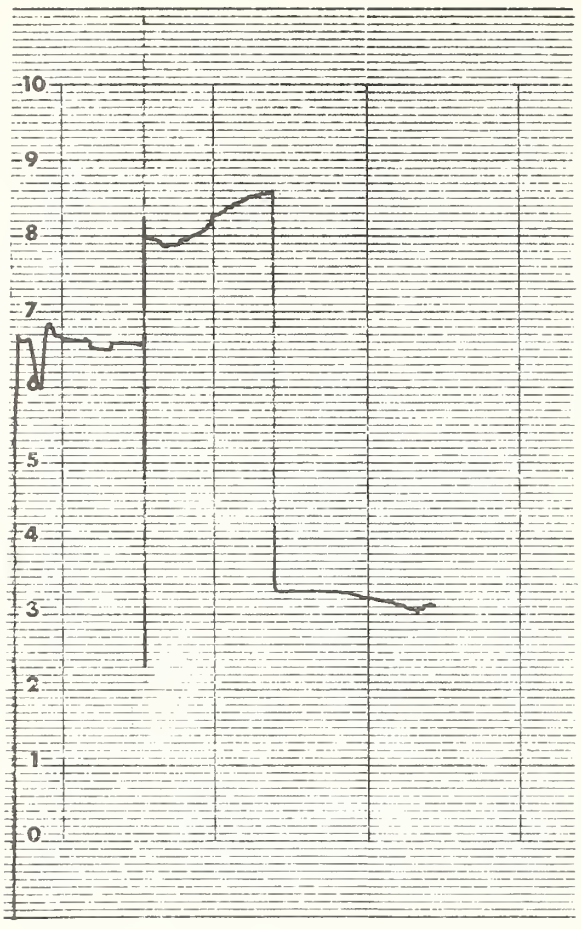

Figure 4-9. Chart recording of silicon layer profile from a surface profilometer. Scale is 2 x 10^4 per major division.

wavelength of the transmittance minimum (V) and maximum (P). The calculated thickness is 1.1379 μm. To check this thickness determination, a surface profilometer was used. A portion of the silicon layer was etched from the substrate to form a step, required for a thickness determination. The surface profilometer employs a chart recorder to display the profile of the surface as a diamond stylus is mechanically drawn across the sample. Figure 4-9 is a portion of this record. The step height determined from this record is 1.05 μm. The agreement is then 8.4 percent, a reasonable value for a profilometer.

5. Results for a-Si:H

The measurement method described in section 3 and applied to epitaxial silicon on sapphire in section 4 is now applied to hydrogenated amorphous silicon deposited on sapphire by the glow-discharge method [13]. The refractive index results are tabulated and compared with the refractive index of epitaxial silicon and of a-Si:H [14]. The model for a modulator structure is

presented and the inconsistency which appears is examined. The required change in refractive index is then determined from some preliminary optical modulation data. A more detailed and complete description of the optical modulation capabilities of a-Si:H will be presented in a paper to be published by others.

5.1 Refractive Index of a-Si:H

A sample [15] of a-Si:H was prepared by the glow discharge technique. This technique involves exciting a plasma via an RF antenna in a chamber containing silane (SiH_4) gas. The silane decomposes to silicon and hydrogen and the silicon deposits with some hydrogen on a heated substrate in the chamber. The substrate is a sapphire wafer and is kept at approximately 250°C during the deposition.

The sapphire wafer used was polished on both sides by the manufacturer; this facilitated the desired optical transmission measurements. The same experimental procedure is followed for a-Si:H sample as for the SOS sample. Figures 5-1 and 5-2 contain the incident (I), transmitted (T) and transmittance (T) spectra of a-Si:H on sapphire from 0.6 to 1.2 μm and from 1.0 to 1.6 μm respectively. The source is filtered by a red plastic filter for the 0.6 to 1.2 μm spectrum and a silicon wafer which has been polished on both sides for the 1.0 to 1.6 μm spectrum. The filters block the harmonics coming through the grating monochrometer. A layer thickness of 1.150 ± 0.002 μm was determined using eq (3.11). In figure 5-1, absorption effects are seen by a decrease in the transmittance peak at 0.821 μm from the value predicted by eq (3.12) and these effects increase dramatically as the 0.6 μm wavelength is approached. The computer aided iterative method is used to find n and k for the 0.6 to 0.821 μm region. The results are presented in table 5.1. The values presented in table 5.1 are used to calculate, via linear interpolation, the real part of the refractive index at other wavelengths for comparison with the real part of the refractive index of a-Si:H determined by Zanzucchi et al. [14]. The results of Zanzucchi's work indicate that the substrate temperature maintained during the silicon deposit effects the refractive index of the silicon. Table 5.2 presents Zanzucchi's results for two samples prepared with substrate temperatures which bound the substrate temperature used in the preparation of the sample examined in here. The real part of the refractive index for this material is also bounded by that of Zanzucchi.

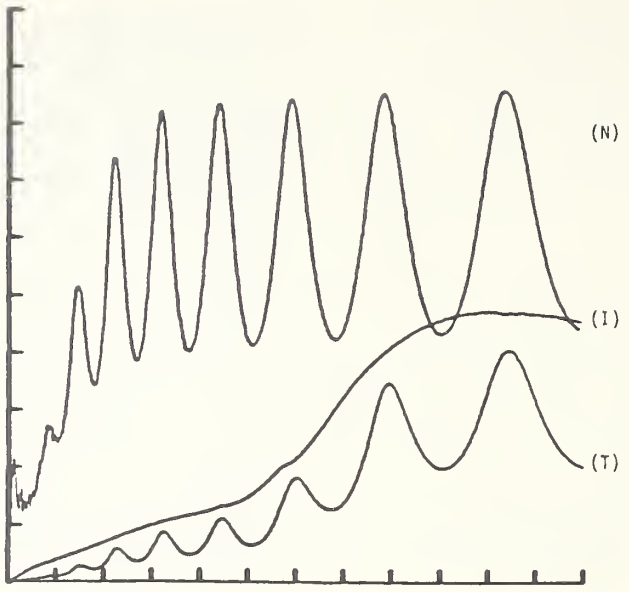

Figure 5-1. (I) incident, (T) transmitted, and (N) transmittance spectra for a-Si:H and sapphire for 0.6 to 1.2 μm. Transmittance (N) full scale is 100 percent.

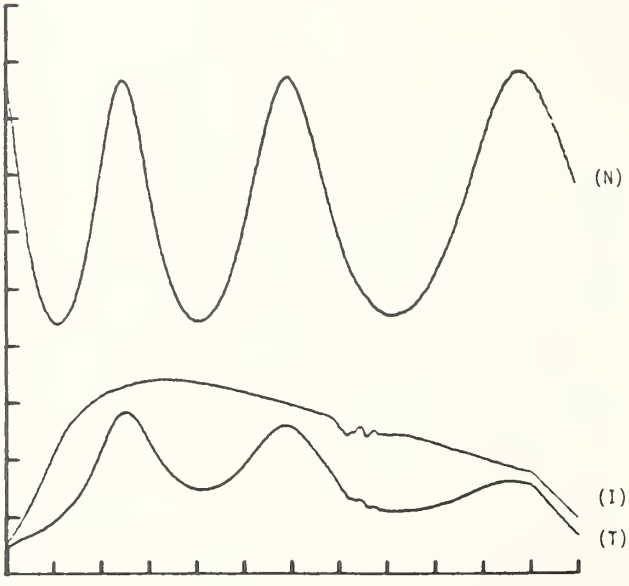

Figure 5-2. (I) incident, (T) transmitted, and (N) transmittance spectra for a-Si:H and sapphire for 1.0 to 1.6 μm. Transmittance (N) full scale is 100 percent.

Table 5.1

Experimental Results of the Refractive Index of a-Si:H

λ	n	k
0.673	3.8090	0.017
0.693	3.7714	0.0108
0.712	3.7198	0.005
0.737	3.6899	0.003
0.761	3.6444	0.001
0.790	3.6114	0.0008
0.821	3.5744	0.0005
0.857	3.5445	0.0003
0.898	3.5186	0.0001
0.944	3.5077	0
0.996	3.4690	0
1.055	3.4448	0
1.124	3.4255	0
1.204	3.3967	0
1.298	3.3802	0
1.405	3.3539	0
1.541	3.3442	0

Table 5.2

Comparison of the Real Part of the Refractive Index

λ	195°C a-Si:H (Z)	250°C a-Si:H (L)	325°C a-Si:H (Z)
0.65	3.77	3.85*	3.99
0.7	3.68	3.7524	3.88
0.75	3.60	3.6653	--
0.8	3.50	3.5995	3.66
0.85	3.40	3.5503	3.69
0.9	3.40	3.5181	3.70
0.95	3.40	3.5032	--
1.00	3.36	3.4674	3.76

*extrapolated

(L) This work

(Z) Zanzucchi et al., [14]

5.2 A Model for the Modulator Structure: Evidence of Gold-Silicon Interaction

To determine the change in refractive index with applied electric field, the transmittance of the modulator structure must be modeled.

The modulator consists of a layer of a-Si:H sandwiched by two gold electrode layers with a sapphire substrate. The modulator is seen to be a stratified thin film device and the model examined in section 2 can be applied. The refractive indices and thickness of the a-Si:H were determined in section 5.1, the refractive indices of the gold layers were determined as outlined in section 4 and sapphire substrate indices were taken from the literature. The thicknesses of the gold layers were taken from the crystal thickness monitor and then adjusted to produce the proper transmittance amplitudes as discussed in section 4. Figure 5-3 is a plot of the expected transmittance spectrum for the wavelength region from 0.6 to 1.2 micrometers. Figure 5-4 is the actual transmittance spectrum of the modulator. The amplitudes of the maxima are down by a factor of two from the expected value.

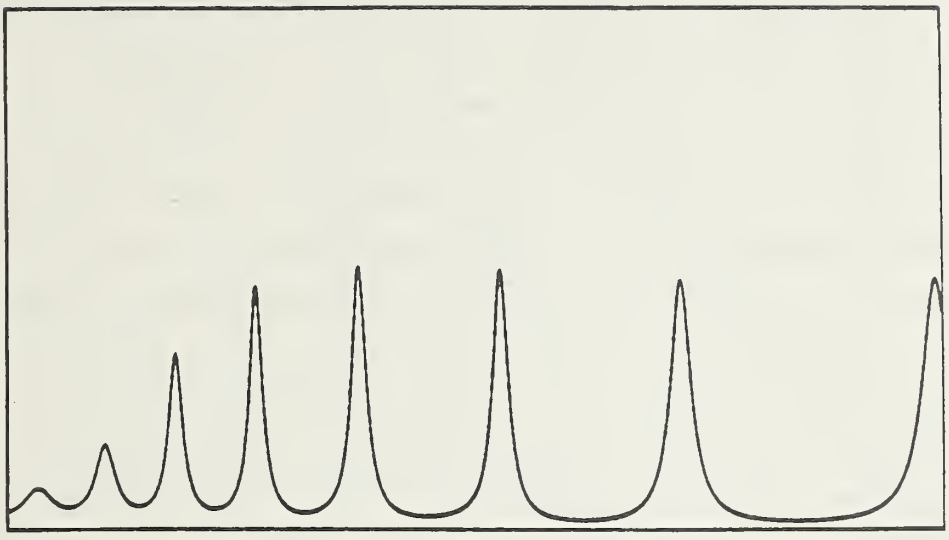

Figure 5-3. Calculated transmittance spectrum of the modulator structure from 0.6 to 1.2 μm. Full scale is 100 percent.

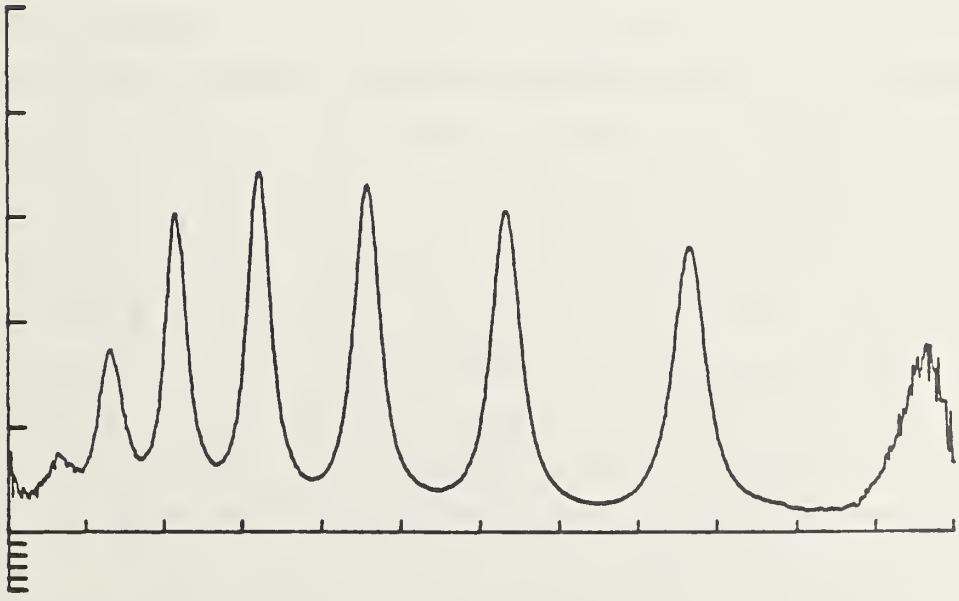

Figure 5-4. Experimental transmittance spectrum of the modulator from 0.6 to 1.2 μm. Full scale is 30 percent.

Two possible causes of this reduction in transmittance became apparent in a search of the literature. Chopra [16] and Knights [17] describe surface roughness in gold and a-Si:H films, respectively. The roughness is due to the deposition techniques used for these two materials. Knights also states that the a-Si:H layer may be anistropic due to variations in the amount of hydrogen incorporated during deposition. A rough surface would cause scattering of the incident light and reduce the measured transmittance. A study done by Hiraki [18] on crystalline silicon reveals that the silicon migrates through the gold layer and forms silicon crystallites in the gold layer. The net effect would again be an increased scattering and reduced transmittance. Hiraki's study of silicon and gold also indicated that the gold will migrate into the silicon at room temperature. The gold is then a dopant and would increase the absorption in the silicon.

Two possible corrections to the device model are suggested by the above discussion of Hiraki's work. The first is to average the transmittance of the device over a variation in the gold and a-Si:H thicknesses, but keeping the sum of the three thicknesses constant. The other possible correction is an increase in the imaginary part of the refractive index of the a-Si:H to introduce more absorption.

The effectiveness of these two corrections can be measured by the resulting reduction in peak transmittance to the experimental values and a preservation of the shape of the resulting transmittance spectrum. Since the a-Si:H layer sandwiched by two gold layers forms a Fabry-Perot interferometer, the shape of the transmittance spectrum can be termed "the device finesse."

Figure 5-5 is a theoretical plot of the transmittance spectrum of another modulator device. The plot was generated by averaging 15 transmittance spectra. The thickness of the a-Si:H and gold layers were varied but their combined sum was kept constant for each of the 15 spectra. A weighting system was used to approximate a Gaussian thickness distribution. When figure 5-5 is compared with figure 5-4, it is seen that both the peak amplitude and the finesse are in good agreement.

Figure 5-6 is a theoretical plot of the transmittance spectrum of the modulator device in which the a-Si:H absorption is increased by increasing k, the imaginary part of the refractive index. Figure 5-6 also compares well with figure 5-4 in both peak transmittance and finesse.

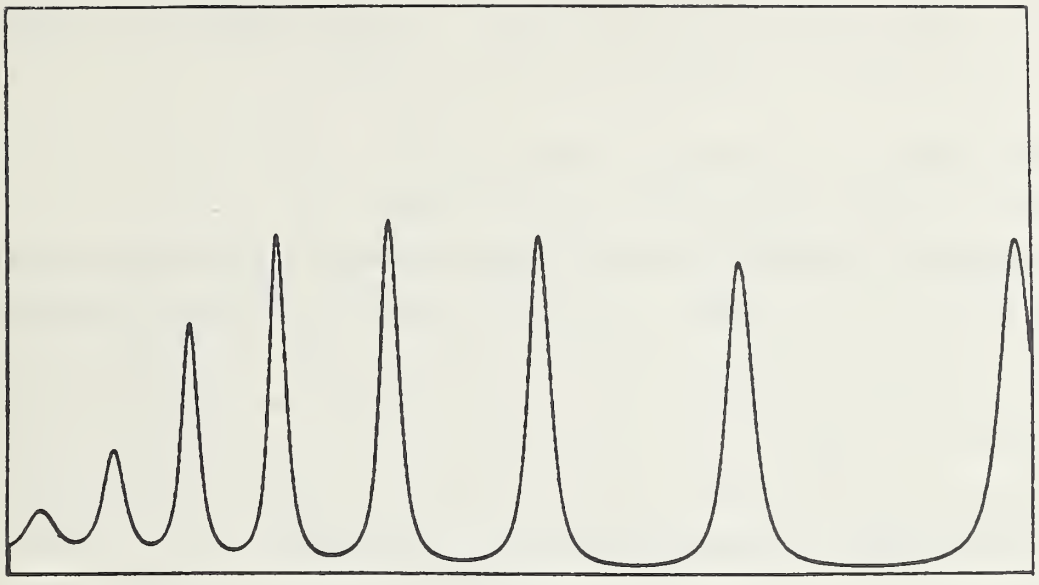

Figure 5-5. Calculated transmittance spectrum of the modulator structure from 0.6 to 1.2 μm. Fifteen thicknesses averaged. Full scale is 30 percent.

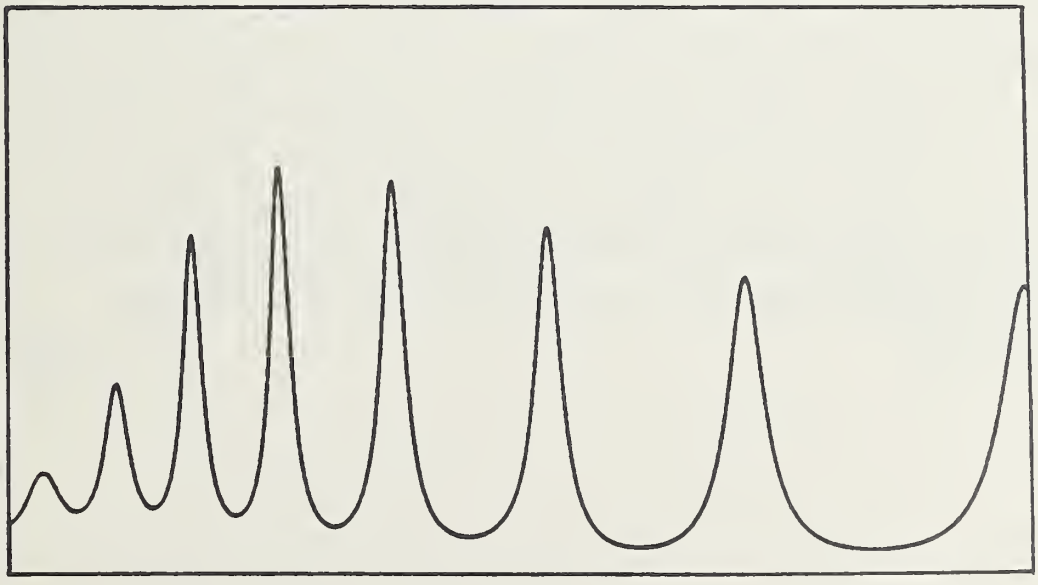

Figure 5-6. Calculated transmittance spectrum of the modulator structure from 0.6 to 1.2 μm, k for a-Si:H increased over previously measured value. Full scale is 30 percent.

Since increasing the k for a-Si:H produces acceptable results and uses much less computer time, it will be used in the next section as a model for determining a change in refractive index of a-Si:H.

5.3 Determination of the Change in Refractive Index of a-Si:H with Applied Electric Field

The model developed in section 3 and corrected in the previous section is used to determine the change in refractive index of a-Si:H with applied electric field. This is done by assuming a change in index and calculating a modulation spectrum using eq (3.13). The calculated and experimental modulation spectra are compared and the magnitude of the index change is adjusted to increase the agreement between the calculated and actual spectra. This iteration continues until the desired agreement is achieved.

Figure 5-7 is a plot of an experimental modulation spectrum. This is obtained by using the same procedure as outlined in section 4, but with the "lock-in" amplifier tied to a voltage pulse applied to the modulator as opposed to being tied to a mechanical chopper. The transmission spectrum is recorded and the pulse train from the lock-in is switched from the modulator to the chopper and a transmission spectrum is again recorded. The ratio of modulated to chopped transmission spectra forms the modulation spectrum. Figure 5-8 is a plot of the calculated modulation spectrum after adjustment for acceptable agreement with experiment. Table 5.3 contains the required change in refractive index and is compared to several other electro-optic materials as tabulated by Hammer [19]. As expected, a change in k produces an amplitude modulation and a change in n produces a phase modulation. In the spectral region from 0.6 to 0.8 μm; the change in k dominates while from 0.8 to 1.2 μm, k is approximately zero and the change in n dominates.

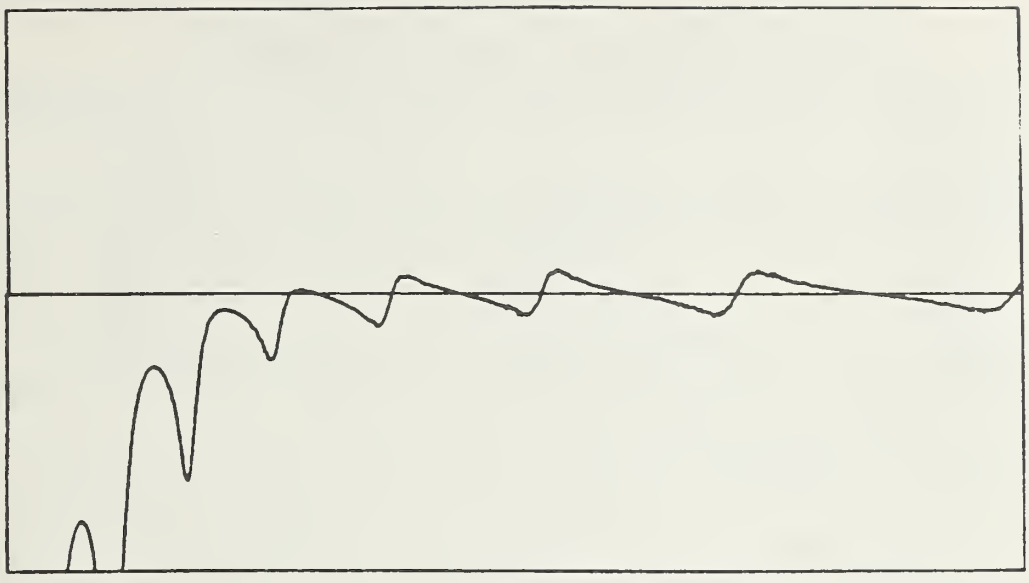

Figure 5-7. Calculated modulation spectrum from 0.6 to 1.2 μm. Full scale is ± 0.2 percent.

Figure 5-8. Experimental modulation spectrum from 0.6 to 1.2 μm. Full scale is ± 0.2 percent.

Table 5.3

Change in Refractive Index of Four Materials

Material	Δn	Δk
a-Si:H	1×10^{-6}	1.75×10^{-3}
Z_nO	1.1×10^{-5}	not given
GaAs	2.8×10^{-5}	not given
$LiNbO_3$	1.6×10^{-4}	not given

Applied field $E = 10^6$ V/m

6. Conclusions

As was pointed out in sections 3 and 5, eq (3.12) provides a means of determining the quality of a measurement. The transmittance maxima obtained experimentally, in regions where eq (3.12) holds, can be compared to the result of eq (3.12) and the error between these two values, will be the approximate error in the T_{ave} (min) amplitude measurement. An error of ± 2 percent in T_{ave} (min) will yield an error of ± 1.3 percent in the value of n_1 (assuming the index of sapphire, n_2, is 1.7500). In calculating the thickness of the layer from eq (3.11), another source of error is in the determination of the wavelength of the extrema. An error of ± 0.5 percent in the wavelength of the transmittance extremum determination will produce an error of ± 0.5 percent in the thickness. These two errors produce a 1.8 percent error in the calculation of the index at other wavelengths when eqs (3.6) and (3.7) are used to do so. Appendix C also gives an indication of the measurement error introduced by assuming the material is nondispersive. It has also been pointed out that the value for refractive index, n_1, calculated from eq (3.10) is not dependent on the wavelength of the minimum, the order of the minimum or the layer thickness. These two points are the main attributes of the measurement method. Since the values of refractive index obtained in section 4 for SOS are in good agreement with published values, it can be concluded that the measurement method produces reasonable results. The transmittance model revealed a significant interaction between gold and a-Si:H, an interaction which was not previously suspected.

7. References

[1] Johnk, Carl T. A. Engineering electromagnetic fields and waves. New York: Wiley; 1975. 377-383.

[2] Azzam, R. M. A.; Bashara, N. M. Ellipsometry and polarized light. Amsterdam: North-Holland; 1977. 332-340.

[3] Johnk, Carl T. A. Op. cit., 378.

[4] Azzam, R. M. A.; Bashara, N. M. Op. cit., 283.

[5] Goodman, Alvin M. Optical interference method for the approximate determination of refractive index and thickness of a transparent layer. Applied Optics 17:2779-2787; 1978 October 1.

[6] Denton, R. E.; Campbell, R. D.; Tomlin, S. G. The determination of the optical constants of thin films from measurements of reflectance and transmittance at normal incidence. J. Physics, D: Applied Physics 5:852-863; 1972.

[7] Malitson, Irving H. Refraction and dispersion of synthetic sapphire. J. Opt. Soc. Amer. 52:1377-1379; 1962 December.

[8] Wise, Edmund M. Gold, recovery, properties and applications. Princeton: Van Nostrand; 218-219; 1964.

[9] Weiss, K. Optische Konstanten dicker metallschichten. Z. Naturforsch 3a:143; 1948.

[10] Heavens, O. S. Optical properties of thin solid films. New York: Academic Press; 200; 1955.

[11] Hulthen, Rolf. Optical constants of epitaxial silicon in the region 1-3.3 eV. Physica Scripta 12:342-344; 1975.

[12] Kühl Ch.; Schlötterer, H.; Schwidefsky, F. Optical investigation of different silicon films. J. Electrochem. Soc.: Solid-State Science and Technology 121:1496-1500; 1974 November.

[13] Chittick, R. C.; Alexander, J. H.; Sterling, H. F. The preparation and properties of amorphous silicon. J. Electrochem. Soc. 116:77-81; 1969.

[14] Zanzucchi, P. J.; Wronski, C. R.; Carlson, D. E. Optical and photoconductive properties of discharge-produced amorphous silicon. J. Appl. Phys. 48:5225-5236; 1977.

[15] Prepared by Paul Werner of the Electromagnetic Technology Division of the National Bureau of Standards.

[16] Chopra, Kasturi L. Thin film phenomena. New York: McGraw-Hill; 1969. 164.

[17] Knights, J. C. Growth morphology and defects in plasma-deposited a-Si:H. J. Non-Crystaline Solids 35&36:159-170; 1980.

[18] Hiraki, A. Low temperature migration of silicon through gold film in Si-Au system. Progress in the Study of Point Defects. Doyama, Yoshida, eds. Tokyo: Univ. of Tokyo Press; 1977. 393-440.

[19] Hammer, J. M. Topics in applied physics. Integrated Optics. Tamir, ed. New York: Springer-Verlag; 1975. 150.

Appendix A. FORTRAN Implementation of the Transmittance Model

```
      PROGRAM SILICON (INPUT,OUTPUT,TAPE2=OUTPUT)
C     THIS MODELS THE TRANSMISSION AND REFLECTION OF LIGHT INCIDENT
C     ON A MULTILAYERED,THIN FILM STRUCTURE WITH A TRANSPARENT SUBSTRATE.
C     SCATTERING MATRIX IS EMPLOYED AND THE RESULT HAS BEEN AVERAGED
C     OVER THE SUBSTRATE THICKNESS.  FOR A NON-NORMAL ANGLE
C     OF INCIDENCE, PERPENDICULAR OR PARALLEL POLARIZATION MAY BE SELECTED.
C
C
C     RESULTS DISPLAYED BY PLOT10 (TEKTRONIX)
C
C
C     LAYER PARAMETERS INPUT INTO ARRAY P(LAYERS,L,5)
C     IN FORMAT N=N1*L+N2,K=K1*L+K2:,D=THICKNESS N1,N2,K1,K2,D
C
C
      COMPLEX S(2,2,2),R(2,6),E(6),T(2,6),ANGLE(4),W
      COMPLEX T1,T2,T3 R1,R2,R3,A(2,2,2),DP DS,N(4)
      COMPLEX TO,IMAG,ECON(4)
      DIMENSION NKDATA (4),TEF(48)
      DIMENSION P(4 9,6),REF(4,30)
C
C
C     AIR,AMORPHOUS SILICON,SAPPHIRE,AIR
C
C
C     ENTER THICKNESS'
C
      DATA P(1,1,6),P(2,1,6),P(3,1 6)/0 0,1.0E-6,6.35E-4/
      DATA P(4,1,6)/0 /
C
C     ENTER INDEX DATA: WAVELENGTH N,K
C
      DATA NKDATA/2 10,2,2/
     DATA TEF/6E-7 1.,0.,1.2E-6,1.,0.,
     #6E-7,3.95,.06,6.5E-7,3.9,.032,7E-7,3.812,.01,
     #7.5E-7,3.716,2.75E-3,8E-7 3.64,1.12E-3,8 5E-7,3.597 .00018
     #9E-7,3.563 0.,
     #9 5E 7,3 537,0.,1E-6 3.516,0.0,1.25E-6 3.45,0.0,
     #6E-7,1.74,0.,1.2E-6,1.76,0.,6E-7 1.,0.,
     #1.2E-6,1.,0./
C
C    FUNCTION DEFINITIONS
C
      U(C B)=(SQRT(B*B+(1+C)**2)-SQRT(B*B+(1-C)**2))/2
      V(C,B)=(SQRT(B*B+(1+C)**2)+SQRT(B*B+(1-C)**2))/2
      RSIN(C,B)=ATAN(U(C,B)/SQRT(1-U(C B)*U(C.B)))
      AIMSIN(C,B)=ALOG(V(C,B)+SQRT(V(C B)* 2-1))
      LAYERS=2
      LAY2=LAYERS+2
      LAY1=LAYERS+1
C
C    DEFINE CONSTANTS (SQRT(-1) AND PI)
C
      IMAG=CMPLX(0 ,1.)
      PI=3.1415926
C
C     FILL THE P MATRIX
C
      K=1
      DO 30 I=1,LAY2
       NKD=3*NKDATA(I)
        DO 20 J=1,NKD
         REF(I,J)=TEF(K)
         K=K+1
20       CONTINUE
30      CONTINUE
?
```

```
       NKDMAX=1
       DO 50 J=1,LAY2
        NKD=NKDATA(J)-1
        IF (NKD .GE. NKDMAX)NKDMAX=NKD
         K=1
        DO 40 I=1,NKD
         P(J,I,1)=REF(J,K+3)
         P(J,I,2)=(REF(J,K+1)-REF(J K+4))/(REF(J,K)-REF(J,K+3))
         P(J,I,3)=REF(J K+1)-P(J,I,2)*REF(J,K)
         P(J,I,4)=(REF(J,K+2)-REF(J,K+5))/(REF(J,K)-REF(J K+3))
         P(J,I,5)=REF(J,K+2)-P(J,I,4)*REF(J,K)
         K=K+3
40      CONTINUE
50     CONTINUE
C
C     FILL REST OF P
C
        DO 90 I=2,NKDMAX
         DO 80 J=1,6
          P(1,I,J)=P(1,1,J)
          P(2,I,6)=P(2 1,6)
          P(3,I,J)=P(3,1,J)
          P(4,I,J)=P(4,1,J)
80       CONTINUE
90      CONTINUE
C
C   DEFINE THE COMPLEX ARCSIN=ARCSIN(REAL,IMAGE)
C
C   SET UP FOR PLOT-10 AND FRAME THE PLOT
C
       CALL INITT (960)
       CALL TERM (3,4096)
       CALL DWINDO(0.,1023 ,0.,1023.)
       CALL CHRSIZ (4)
       CALL MOVEA(0.,0.)
       CALL DRAWA(0 ,590 )
       CALL DRAWA(816.,590.)
       CALL DRAWA(816.,0 )
       CALL DRAWA(0.,0.)
C
C  ********** PLOT THE SPECTRUM **********
C
C    K IS A DATA POINTER
C
       K=1
       DO 1000 M=1,601
        WAVE=.599E-6+1E-9*M
        IF(WAVE.GT.P(2,K,1)) K=K+1
        DO 100 I=1,LAY2
         ABSORP=-1*(P(I,K,4)*WAVE+P(I,K,5))
C  THE COMPLEX REFRACTIVE INDEX FOR LAYER I
         N(I)=CMPLX(P(I,K,2)*WAVE+P(I,K,3),ABSORP)
100      CONTINUE
C    ANGLE(1)=INCIDENT ANGLE
       ANGLE(1)=CMPLX(0.,0.)
       DO 110 I=2,LAY2
        W=N(I-1)*CSIN(ANGLE(I-1))/N(I)
        C=REAL(W)
        B=AIMAG(W)
        C1=RSIN(C B)
        B1=AIMSIN(C,B)
        ANGLE(I)=CMPLX(C1,B1)
110     CONTINUE
?
```

```
C     CALCULATE THE INTERFACE AND LAYER MATRICES' ELEMENTS
C      * R,T,EXP(JB),EXP(-JB) *
         DO 200 I=2,LAY2
          DP=N(I)*CCOS(ANGLE(I-1))+N(I-1)*CCOS(ANGLE(I))
          DS=N(I-1)*CCOS(ANGLE(I-1))+N(I)*CCOS(ANGLE(I))
          R(1,I)=(N(I)*CCOS(ANGLE(I-1))-N(I-1)*CCOS(ANGLE(I)))/DP
          R(2,I)=(N(I-1)*CCOS(ANGLE(I-1))-N(I)*CCOS(ANGLE(I)))/DS
          T(1,I)=2*N(I-1)*CCOS(ANGLE(I-1))/DP
          T(2,I)=2*N(I-1)*CCOS(ANGLE(I-1))/DS
          E(I)=CEXP(IMAG*2*PI*N(I)*CCOS(ANGLE(I))*P(I,1,6)/WAVE)
          ECON(I)=CEXP(CONJG(IMAG)*2*PI*N(I)*CCOS(ANGLE(I))
     #*P(I,1,6)/WAVE)
200      CONTINUE
C
C  *** CALCULATE SCATTERING MATRIX ***
C
         DO 210 I=1,2
          S(I,1,1)=1/T(I,2)
          S(I,1,2)=R(I,2)/T(I,2)
          S(I,2,1)=S(I,1,2)
          S(I,2,2)=S(I,1,1)
210      CONTINUE
         DO 300 I=3,LAY1
          DO 275 J=1,2
           A(J,1,1)=(S(J,1,1)*E(I-1)+S(J,1,2)*R(J,I)*ECON(I-1))/T(J,I)
           A(J,1,2)=(S(J,1,1)*R(J,I)*E(I-1)+S(J,1,2)*ECON(I-1))/T(J,I)
           A(J,2,1)=(S(J,2,1)*E(I-1)+S(J,2,2)*R(J,I)*ECON(I-1))/T(J,I)
           A(J,2,2)=(S(J,2,1)*R(J,I)*E(I-1)+S(J,2,2)*ECON(I-1))/T(J,I)
           DO 250 L1=1,2
            DO 225 L2=1,2
             S(J,L1,L2)=A(J,L1,L2)
225         CONTINUE
250        CONTINUE
275       CONTINUE
300      CONTINUE
C
C    *** CALCULATE TAVE AND RAVE ***
C
C     SELECT DESIRED POLARIZATION
C     J=1 FOR PAR,J=2 FOR PER
         J=2
C
         T0=N(LAY1)*CCOS(ANGLE(LAY1))/(N(1)*CCOS(ANGLE(1)))
         T1=1.0/(S(J,1,1)*CONJG(S(J,1,1)))
         T2=T(J,LAY2)*CONJG(T(J,LAY2))
         T3=T1*T0*CONJG(T0)
         R1=T1*S(J,2,1)*CONJG(S(J,2,1))
         R2=R(J,LAY2)*CONJG(R(J,LAY2))
         R3=S(J,1,2)*CONJG(S(J,1,2))*T1
         TAVE=REAL(T1*T2/(1-R2*R3))
         RAVE=REAL((R1-R1*R2*R3+T1*T3*R2)/(1-R2*R3))
C
C     PLOT TAVE
C
        Y=590.0*TAVE
        X=1.36E9*(WAVE-.6E-6)
        CALL DRAWA(X,Y)
1000    CONTINUE
        CALL FINITT (0.,0.)
        STOP
        END
 -END OF FILE-
?
```

Appendix B. Derivation of Equation (3.9)

The following equations model the structure depicted in figure B-1.

$$T_{ave} = T_1 T_2 / [1 - R_2 R_3],$$

where

$$T_1 = 1/(S_{11} S_{11}^*),$$

$$T_2 = t_{23} t_{23}^*,$$

$$R_2 = r_{23} r_{23}^*,$$

$$R_3 = S_{12} S_{12}^* / (S_{11} S_{11}^*);$$

and

$$S = I_{01} L_1 I_{12},$$

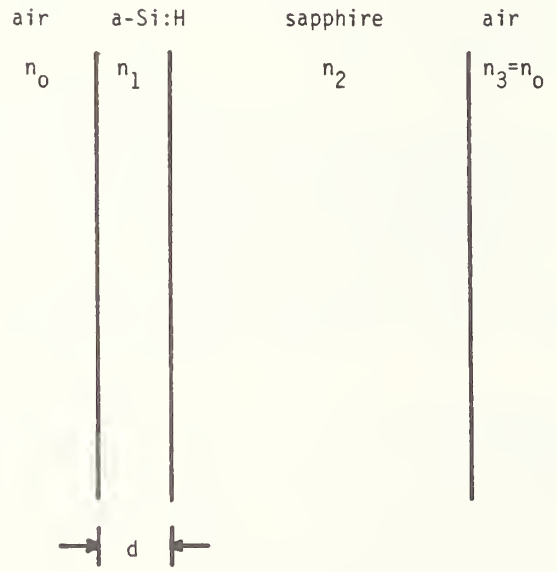

Figure B-1. System modeled in appendix B.

where

$$I = \frac{1}{t} \begin{bmatrix} 1 & r \\ r & 1 \end{bmatrix},$$

and

$$L = \begin{bmatrix} e^{J\beta} & 0 \\ 0 & e^{-J\beta} \end{bmatrix} \quad \text{with } \beta = 2\pi\, Nd/\lambda\ .$$

This implies that:

$$S = \frac{1}{t_{01}t_{12}} \begin{bmatrix} 1 & r_{01} \\ r_{01} & 1 \end{bmatrix} \begin{bmatrix} e^{j\beta_1} & 0 \\ 0 & e^{-j\beta_1} \end{bmatrix} \begin{bmatrix} 1 & r_{12} \\ r_{12} & 1 \end{bmatrix},$$

resulting in:

$$S_{11} = (e^{j\beta_1} + r_{01}r_{12}\, e^{-j\beta_1})/(t_{01}t_{12})$$

and

$$S_{11} = (r_{12}\, e^{j\beta_1} + r_{01}\, e^{-j\beta_1})/(t_{01}t_{12})\ .$$

Since we assume that $k_1 = 0$,

$$\beta_1 = 2\pi\, n_1 d_1/\lambda,$$

$$t_{01} = 2n_0/(n_0+n_1),$$

$$t_{12} = 2n_1/(n_1+n_2),$$

$$r_{01} = (n_0-n_1)/(n_0+n_1),$$

and

$$r_{12} = (n_1-n_2)/(n_1+n_2) .$$

Therefore,

$$T_1 = 16n_0^2n_1^2/[(n_0+n_1)^2(n_1+n_2)^2 + (n_0-n_1)^2(n_1-n_2)^2$$

$$+ 2(n_0^2-n_1^2)(n_1^2-n_2^2) \cos (4\pi n_1 d_1/\lambda)] = 16n_0^2n_1^2/B,$$

$$R_3 = [(n_0+n_1)^2(n_1-n_2)^2 + (n_0-n_1)^2(n_1+n_2)^2$$

$$+ 2(n_0^2-n_1^2)(n_1^2-n_2^2) \cos (4\pi n_1 d_1/\lambda)]/B,$$

and for a lossless substrate, $k_2 = 0$, so

$$T_2 = 4n_2^2/(n_2+n_3)^2 = 4n_2^2/(n_2+n_0)^2,$$

and

$$R_2 = [(n_2-n_0)/(n_2+n_0)]^2 .$$

The cosine term in the expressions for T_1 and R_3 may be simplified since we are assuming that T_{ave} is at a minimum or valley point. At a valley, assuming n_1 is greater than n_2,

$$2n_1 d_1 = (m + 1/2)\lambda_V \quad m = 1, 2, \cdots.$$

Therefore,

$$\cos(4\pi n_1 d_1/\lambda) = \cos ((2m+1)\pi) = -1 ,$$

since 2m+1 is an odd integer. This allows the expression for T_{ave} to be simplified greatly.

$$T_{ave}(\lambda_V) = T_V = 4n_0n_1^2n_2/[n_0^2n_1^2+n_0^2n_2^2+n_1^4+n_1^2n_2^2] \ .$$

The known or measured values are n_0, n_2 and T_{ave} (λ_V), so the equation can be solved for n_1.

$$n_1 = \{-(n_0^2-4n_0n_2/T_v + n_2^2)/2 + [n_0^2-4n_0n_2/T_v + n_2^2)^2 - 4n_0^2n_2^2]^{1/2}/2\}^{1/2}$$

Since

$$d_1 = (m+1/2)\ \lambda_V/(2n_1) \ ,$$

we can determine the thickness d_1 if m is known.

Appendix C. Index Determination Error Resulting From Dispersion

Equation (3.7) was found by making the assumption that the thin layer was both nonabsorbing and nondispersive. The method outlined in section 3 for determining the refractive index incorporates eq (3.10), a result stemming from the use of eq (3.7). The error introduced in the index determination by the probable dispersive nature of the thin film is now examined.

The structure being considered here consists of an unsupported thin film in air (see fig. C-1). The refractive index will be modeled as a linear function of wavelength. The transmittance of this structure is given by eq (C.1).

$$T = \frac{16\ n^2}{(n-1)^4 + (n+1)^4 - 2(n-1)^2(n+1)^2 \cos\ (4\pi nd/\lambda)} \qquad (C.1)$$

Assuming the index n is changing with wavelength λ, the transmittance extrema is found by letting the derivative of the transmittance with respect to wavelength go to zero. This is given by eq (C.2).

Figure C-1. Structure modeled by eq (C.1).

$$\frac{\partial T}{\partial \lambda} = \frac{16\ nA\ \partial n/\partial \lambda - 8n^2(B-C)}{A^2}, \qquad (C.2)$$

where

$$A = n^4 + 6n^2 + 1 - (n^4 - 2n^2 + 1)\cos(4\pi nd/\lambda),$$

$$B = 4n\frac{\partial n}{\partial \lambda}\left[n^2 + 3 - (n^2 + 1)\cos(4\pi nd/\lambda),\right.$$

and

$$C = 4\pi d(n^4 - 2n^2 + 1)\left(\frac{\partial n}{\lambda \partial \lambda} - \frac{n}{\lambda^2}\right)\sin(4\pi nd/\lambda).$$

If $\partial n/\partial \lambda$ is zero, eq (C.3) results.

$$T = \frac{4n^2}{[(n-1)^2 + (n+1)^2]^2} \qquad (C.3)$$

From eq (C.3), the index n may be found from the value of the transmittance, as given in eq (C.4).

$$n = \left[\frac{2 - T + 2(1-T)^{1/2}}{T}\right]^{1/2} \qquad (C.4)$$

For many semiconductors and other optical materials the assumption that $\partial n/\partial \lambda$ is zero is not valid. Equation (C.2) is transcendental and the roots (with respect to wavelength) are found numerically for a fixed $\partial n/\partial \lambda$ using linear bisection. The index n_v and the wavelength at a transmittance minimum (root just determined) are used to find the transmittance using eq (C.1). The value for the transmittance is then used in eq (C.4) to determine an approximate value for the index, n_a. The percent error is then given by

$$\%\ \text{error} = (n_v - n_a)/n_v \times 100\%.$$

Table C.1 contains the percent error for four values of $\partial n/\partial \lambda$. The thickness is 1 μm, the order (heading), index, and $\partial n/\partial \lambda$ (right column, index change per meter) are also given. All calculations were performed to 12 decimal places. As can be seen in the table, the worst error is for a $\partial n/\partial \lambda$ of -1.0 E+06 at the 1.5 order minimum. This error of 1 percent occurs at a unrealistic value of dispersion and wavelength for nearly all optical materials but is still less than the probable experimental error in any transmittance measurements.

It can be concluded from an examination of table C.1, that the approximation ($\partial n/\partial \lambda = 0$) introduces negligible error into the index determination made in this work.

Table C-1.
Percent error introduced into refractive index
calculation for listed values of index, order (m)
and dispersion ($\partial n/\partial \lambda$, λ in meters)

	1.5	2.5	3.5	4.5	5.5	6.5	7.5	8.5	
Index	3.812	3.803	3.750	3.734	3.710	3.700	3.700	3.694	+5.0E+04
% error	1.3E-02	1.6E-03	4.1E-04	1.5E-04	6.8E-05	3.4E-05	1.9E-05	1.2E-05	
Index	2.054	2.617	2.989	3.249	3.440	3.587	3.703	3.797	-1.0E+06
% error	1.0E+00	2.1E-01	6.8E-02	2.8E-02	1.4E-02	7.7E-03	4.6E-03	2.8E-03	
Index	2.540	3.001	3.264	3.433	3.550	3.636	3.702	3.754	-5.0E+05
% error	4.5E-01	8.1E-02	2.4E-02	9.8E-03	4.6E-03	2.5E-03	1.4E-03	9.0E-04	
Index	3.516	3.605	3.645	3.668	3.683	3.693	3.700	3.706	-5.0E+04
% error	1.0E-02	1.4E-03	3.7E-04	1.4E-04	6.2E-05	3.2E-05	1.8E-05	1.1E-05	

U.S. DEPT. OF COMM. BIBLIOGRAPHIC DATA SHEET (See instructions)	1. PUBLICATION OR REPORT NO. NBSIR 81-1652	2. Performing Organ. Report No.	3. Publication Date December 1981

4. TITLE AND SUBTITLE

A Measurement Method for Determining the Optical and Electro-Optical Properties of a Thin Film.

5. AUTHOR(S)

Donald R. Larson

6. PERFORMING ORGANIZATION (If joint or other than NBS, see instructions)

NATIONAL BUREAU OF STANDARDS
DEPARTMENT OF COMMERCE
WASHINGTON, D.C. 20234

7. Contract/Grant No.

8. Type of Report & Period Covered

9. SPONSORING ORGANIZATION NAME AND COMPLETE ADDRESS (Street, City, State, ZIP)

10. SUPPLEMENTARY NOTES

☐ Document describes a computer program; SF-185, FIPS Software Summary, is attached.

11. ABSTRACT (A 200-word or less factual summary of most significant information. If document includes a significant bibliography or literature survey, mention it here)

A method of determining the complex refractive index of a thin film on a nonabsorbing substrate is developed. The optical transmittance spectrum of the structure is measured and the index is determined by matching this spectrum numerically. An iterative procedure for finding the magnitude of an induced change in refractive index is also presented. In nonabsorbing spectral regions, the index and film thickness are determined directly.

The optical transmittance of sapphire and thin films of gold and epitaxial silicon, both on sapphire, is examined. The refractive index of epitaxial silicon on sapphire, SOS, is determined and compares favorably with the results of other investigators.

The measurement method is applied to a thin film of hydrogenated amorphous silicon, a-Si:H, deposited by a capacitively coupled rf glow discharge. The index is tabulated for various wavelengths and a field induced change in index comparable to GaAs is measured.

12. KEY WORDS (Six to twelve entries; alphabetical order; capitalize only proper names; and separate key words by semicolons)

Electro-optic modulation; hydrogenated amorphous silicon; optical transmittance; refractive index; scattering matrix; thin film; transmittance extrema.

13. AVAILABILITY

☒ Unlimited

☐ For Official Distribution. Do Not Release to NTIS

☐ Order From Superintendent of Documents, U.S. Government Printing Office, Washington, D.C. 20402.

☒ Order From National Technical Information Service (NTIS), Springfield, VA. 22161

14. NO. OF PRINTED PAGES

65

15. Price

$8.00

USCOMM-DC 6043-P80

☆ U.S GOVERNMENT PRINTING OFFICE: 1982—577-389/110 Region No 8